AFRL-OSR-VA-TR-2013-0143

Deterministic Aperiodic Structures for on-chip Nanophotonics and Nanoplasmonics Device Applications

Luca Dal Negro,
Boston University

April 2013
Final Report

AIR FORCE RESEARCH LABORATORY
AF OFFICE OF SCIENTIFIC RESEARCH (AFOSR)
ARLINGTON, VIRGINIA 22203
AIR FORCE MATERIEL COMMAND

REPORT DOCUMENTATION PAGE

Form Approved
OMB No. 0704-0188

PLEASE DO NOT RETURN YOUR FORM TO THE ABOVE ORGANIZATION.

1. REPORT DATE *(DD-MM-YYYY)*	2. REPORT TYPE	3. DATES COVERED *(From - To)*
01/01/2013	FINAL REPORT	09/01/2009 - 08/31/2012

4. TITLE AND SUBTITLE

Deterministic Aperiodic Structures for on-chip Nanophotonics and Nanoplasmonics Device Applications

5a. CONTRACT NUMBER

5b. GRANT NUMBER
FA9550-10-1-0019

5c. PROGRAM ELEMENT NUMBER

6. AUTHOR(S)

Luca Dal Negro

5d. PROJECT NUMBER

5e. TASK NUMBER
2305J & 3001M

5f. WORK UNIT NUMBER

7. PERFORMING ORGANIZATION NAME(S) AND ADDRESS(ES)

Boston University
25 Buick Street
Boston, MA 02215

8. PERFORMING ORGANIZATION REPORT NUMBER

9. SPONSORING/MONITORING AGENCY NAME(S) AND ADDRESS(ES)

AFOSR
875 N Randolph St
Arlington, VA 22203

10. SPONSOR/MONITOR'S ACRONYM(S)

11. SPONSOR/MONITOR'S REPORT NUMBER(S)
AFRL-OSR-VA-TR-2013-0143

12. DISTRIBUTION/AVAILABILITY STATEMENT

DISTRIBUTION A: APPROVED FOR PUBLIC RELEASE

13. SUPPLEMENTARY NOTES

14. ABSTRACT

During this project the Boston University team developed novel approaches to enhance light-matter coupling in optical devices by engineering photonic-plasmonic resonances in aperiodically ordered nanostructures. In particular, they designed, fabricated and characterized a large number of active photonic nanomaterials and structures and demonstrated unique optical properties such as broadband enhanced local field intensity, scattering, radiative (i.e., light emission) and nonlinear responses (i.e., second harmonic generation, nonlinear refractive index) using Si compatible materials and processing. Fabricated metal-dielectric devices have been integrated with planar Si chips for applications of aperiodic order to light emission, optical sensing, on-chip nonlinear generation, solar energy conversion, and singular optics. The fabrication and experimental characterization of materials and device demonstrators have been partnered with the development of efficient computational design tools based on semi-analytical multiple scattering theory, which allowed the rigorous study and optimization of large-scale aperiodic media for the first time.

15. SUBJECT TERMS

aperiodic systems, nano-optics, plasmonics

16. SECURITY CLASSIFICATION OF:			17. LIMITATION OF ABSTRACT	18. NUMBER OF PAGES	19a. NAME OF RESPONSIBLE PERSON
a. REPORT	b. ABSTRACT	c. THIS PAGE			Luca Dal Negro, Associate Professor
U	U	U	SAR		19b. TELEPHONE NUMBER *(Include area code)* (617) 358-2627

Reset

Deterministic Aperiodic Structures for on-chip nanophotonics and nanoplasmonics device applications, Award FA9550-10-1-0019

Final Report

Luca Dal Negro
Department of Electrical and Computer Engineering & Photonics Center, Boston University, Boston, MA, 02215

Personnel in place: one graduate student worked on this project since the beginning and a post-doctoral associate. The graduate student (Jacob Trevino) will graduate in the Spring 2013 based on the results of this research.

Summary of results: during this project we have developed novel approaches to enhance light-matter coupling in optical devices by engineering photonic-plasmonic resonances in *aperiodically ordered* nanostructures. In particular, we have designed, fabricated and characterized a large number of active photonic nanomaterials and structures and demonstrated unique optical properties such as broadband enhanced local field intensity, scattering, radiative (i.e., light emission) and nonlinear responses (i.e., second harmonic generation, nonlinear refractive index) using Si compatible materials and processing. Fabricated metal-dielectric devices have been integrated with planar Si chips for applications of aperiodic order to light emission, optical sensing, on-chip nonlinear generation, solar energy conversion, and singular optics. The fabrication and experimental characterization of materials and device demonstrators have been partnered with the development of efficient computational design tools based on semi-analytical multiple scattering theory, which allowed the rigorous study and optimization of large-scale aperiodic media for the first time.

Productivity metrics: The many results generated during this project have led to the publication of 32 peer-reviewed journal publications, 4 book chapters, and 1 graduate level textbook (the first on the topic) titled: *Optics of Aperiodic Media,* which will soon be published by Cambridge University Press (see the complete publication list below). The vast range of activities sponsored by this project has also resulted in 27 invited talks, all delivered by Dal Negro at major international conferences in photonics and optical materials, as well as 17 contributed talks delivered by students and postdocs and 18 invited seminars at Universities and leading Scientific Institutions.

Main scientific achievements: design of aperiodic structures

We have designed and engineered aperiodic metal nanoparticle arrays with controllable Fourier spectral properties that interpolate in a tunable fashion between disordered random systems and regular periodic structures.

We refer to this general class of artificial metal-dielectric materials as Deterministic Aperiodic Nano Structures (DANS)[21]. We have demonstrated that these novel aperiodic media, conceived by designing spatial frequencies in aperiodic Fourier space, give rise to characteristic scattering resonances and localized mode patterns that enhance the intensity of optical fields over planar surfaces and broad frequency spectra. Moreover, our work on aperiodic plasmon arrays has unveiled for the first time the distinctive interplay between photonic diffraction and near field plasmonic localization, providing novel opportunities to manipulate light-matter interactions on the nanoscale.

By engineering photonic-plasmonic coupling at multiple wavelengths in aperiodic nanoparticle arrays we have experimentally demonstrated broadband plasmon-enhanced scattering across the entire solar spectrum. By utilizing rigorous electromagnetic design tools [1-3,11,19,23] (i.e., multi-particle generalized Mie theory, Null Field method, Coupled Dipole Theory) we have determined the relevant engineering design rules for the control and enhancement of optical fields in complex aperiodic media, and supported our findings by genetic and particle swarm optimization techniques [3,19]. A number of high impact papers have been published on these topics (see complete list below). Our work has shown that the ability to engineer aperiodic structures in between random and periodic media is important to engineer intense hot spots distributed over large cross sectional areas of the arrays. This point was illustrated by Forestiere et al. [1] who systematically investigated the near-field spectra and far-field scattering response of Ag nanoparticle arrays generated according to prime numbers distributions in two spatial dimensions. Using rigorous coupled-dipole analysis for dipolar nanoparticles, this study demonstrated that significantly increased local field intensity over broad frequency spectra can be obtained by designing closely packed arrays (i.e., large particle filling fractions) and with a large density of spatial frequencies, captured by the arrays spectral flatness[1] (SF).

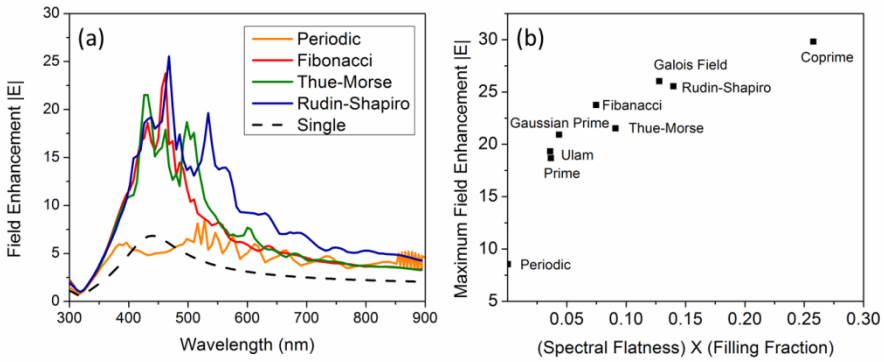

Fig. 1. (a) Maximum field enhancement versus the wavelength for an isolated Ag nanosphere (50nm radius) and for periodic, Fibonacci, Thue-Morse, and Rudin-Shapiro aperiodic arrays of nano-spheres with 50 nm minimum interparticle separation. The arrays are excited by a circularly polarized plane wave at normal incidence. (b) Values of maximum field enhancement versus the spectral flatness (SF) x filling fraction (FF) product for the different arrays indicated in the figure.

This point is also illustrated in Fig. 1(a), where we show the calculated near-field spectra for Ag nanosphere arrays with periodic, Fibonacci, Thue-Morse, and Rudin-Shapiro sequences. The case of a single Ag nanosphere with 50nm radius is also shown for comparison. To better describe the influence of both the polarization states of the incident field, the arrays were excited by a circularly polarized plane wave at normal incidence.
Figure 1(b) demonstrates the scaling behavior of the maximum hot spot field intensity, probed in the plane of the arrays, for a large number of aperiodic deterministic structures

[1]The spectral flatness (SF) is a digital signal processing parameter that measures how spectrally diffused a signal is. In the case of plasmonic structures, the arrays are considered as digitized 2D spatial signals and the SF is calculated by dividing the geometric mean and the arithmetic mean of their Fourier power spectra.

(named in the figure) as a function of the product of the arrays filling fraction (FF) and their Fourier spectral flatness (SF). This plot demonstrates that only aperiodic structures which possess both large spectral flatness SF and nanoparticle filling fraction result in strong plasmonic scattering and near-field plasmonic localization. The rationale for this is that plasmon waves couple very strongly in the near-field regime at very short distances, thus motivating the need of high nanoparticles packing fractions. However, for a given particle density, aperiodic arrays featuring a large number of spatial frequencies can match in-plane scattering processes resulting in efficient multiple scattering in the array plane, and boosting the field enhancement even further. *The coexistence of different electromagnetic coupling regimes at multiple length scales is at the origin of the superior field enhancement and localization observed in several aperiodic plasmonic structures*. Due to the increased structural disorder (spectral flatness), the nanoparticles in the aperiodic arrays are strongly coupled in both the plasmonic near field regime and the photonic diffractive one (long-range coupling), resulting in strong in-plane multiple light scattering. On the other hand, in the case of periodic array the nanoparticles are prevalently coupled in the near-field regime, with strongly reduced phase modulation across the array plane. In this case, extended plasmonic structural resonances, analogous to the Fabry-Perot-type modes in finite-size structures, are formed and decrease the overall field intensity enhancement.

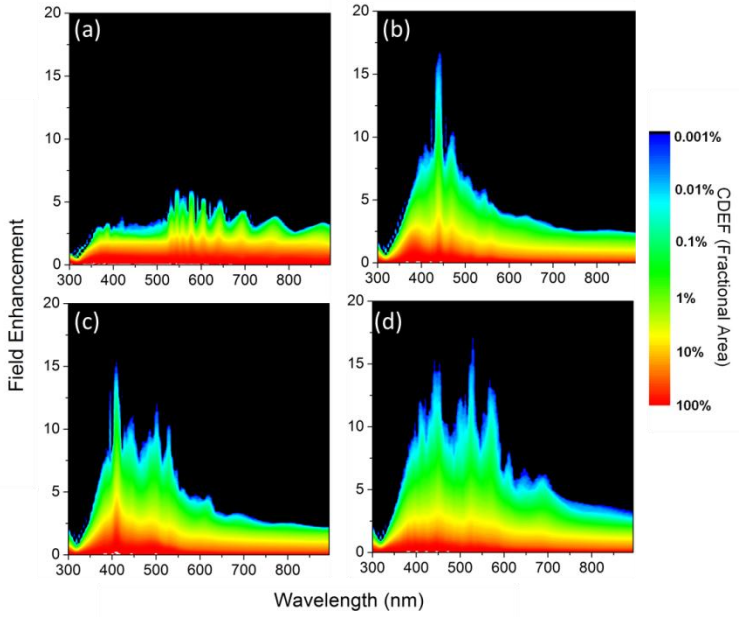

Fig. 2. The color-maps show the cumulative distributions of field enhancement (CDFE) (logarithmic scale) versus wavelength (x-axis) and field-enhancement (y-axis) for (a) Periodic, (b) Fibonacci, (c) Thue-Morse, (d) Rudin-Shapiro. The arrays consist of 50 nm radius Ag spheres with minimum edge-to-edge separations of 25 nm. They are excited by a circularly polarized plane wave at normal incidence.

It is finally to be noticed that aperiodic arrays have been found to perform much better than closely packed periodic ones despite their reduced values of filling fraction. Therefore, the results in Fig. 1 demonstrate clearly that closely-packed aperiodic plasmonic arrays with a large density of spatial frequency are needed in order to enhance the hot spots intensity over a broader frequency range compared to optimized periodic

and quasiperiodic structures. Another important aspect of aperiodic plasmonic arrays that we have discovered is related to the fraction of the total surface area covered by strong plasmonic fields. In plasmonic sensing technology, the control of the areal density of enhanced fields on planar chips is of fundamental importance. In order to quantitatively understand this aspect, we have studied the fraction of the total area of the arrays covered by plasmon enhanced fields with values greater then a fixed threshold value. Mathematically, this can be quantified by introducing the *cumulative distribution of field enhancement* (CDFE), discussed in Ref.[1]

In Fig. 2 we show the calculated CDFE for (a) periodic, (b) Fibonacci, (c) Thue-Morse, and (d) Rudin-Shapiro two-dimensional arrays, respectively. The CDFE function describes the fraction of the total area of these arrays that is covered by enhanced fields with values greater than the value specified in the vertical axis. Although the CDFE does not provide any information about the size of hot spots, it gives a quantitative measure of the spatial distribution of enhanced fields, at each wavelength, with respect to the total surface of the array. The results in Fig. 2 demonstrate that aperiodic arrays with large spectral flatness and particle filling fraction support enhanced field states that are spatially distributed over larger array areas compared to periodic plasmonic structures, which is a very important attribute for the engineering of scattering-based sensors (e.g., SERS substrates) and planar plasmonic devices. However, we should notice here that aperiodic designs with dense Fourier spectra come at the additional cost of a larger system's size compared to narrow-band periodic or multi-periodic structures, ultimately requiring engineering trade-offs between the intensity enhancement, the resonant frequency bandwidth, and the total size of plasmonic devices.

The characteristic behavior of aperiodic nanoplasmonic structures summarized in Figs. 1 and 2 follows from the large number of supported photonic modes available. The large spectral density of photonic resonances distinctive of aperiodic media couple to sub-wavelength localized plasmon modes over a broad frequency range, controlled by the structural complexity of the array. *Broadband hot spots intensity enhancement with aperiodic plasmonic structures is therefore made possible by controlling long-range electromagnetic coupling in multi-scale arrays of resonant nanoparticles with positional fluctuations.*

Another important featured that we discovered in multi-scale electromagnetically coupled aperiodic arrays of metallic nanoparticles is the distinctive scaling of their hot spots intensity with respect to the system's size, or the total number of particles in the array. This is best illustrated by the analytical multiple scattering results shown in in Fig. 3 for Au spheres. Additionally we illustrate the field intensity distribution in the plane of the arrays for periodic square arrays, Fibonacci, Thue-Morse, and Rudin-Shapiro structures.

All the structures are illuminated at normal incidence by a plane wave at 785nm. The distinctive interplay between near-field plasmonic coupling and long-range multiple scattering in aperiodic structures is clearly displayed in Figs. 3(b-d) where we show the electric field spatial distribution at the wavelengths of the enhancement peak. The highly inhomogeneous field distributions in Figs. 3(b-d) demonstrate the importance of long-range multiple scattering effects in the plane of the array, which couple all the particle clusters in the aperiodic arrays. Moreover, when scaling up the size of the arrays by increasing the particles number (Figs. 3e), new configurations of local particle clusters in aperiodic arrays appear separated by wavelength-scale distance, thus increasing the total

number of spatial frequencies in the plane and enhancing the maximum hot spots intensity in a size-dependent fashion.

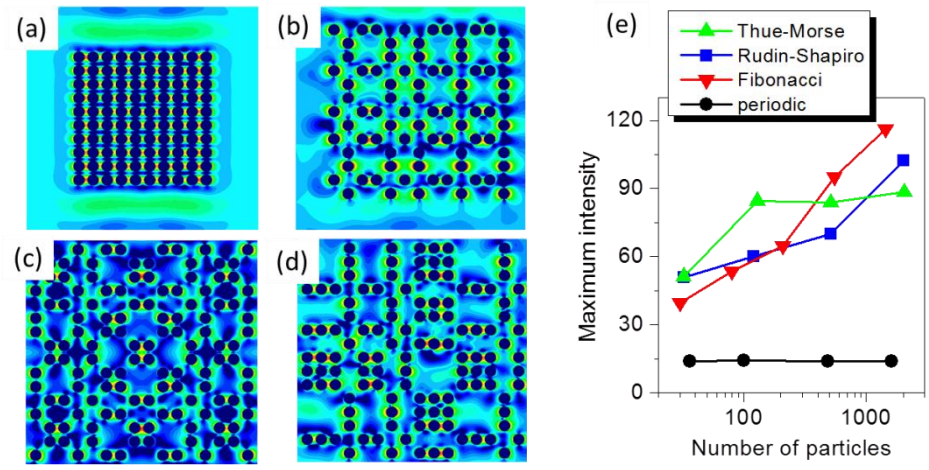

Fig. 3. Generalized Mie Theory (GMT) calculations of electromagnetic field scattered by plasmonic arrays of spherical Au nanoparticles arranged according to (a) a periodic (b) Fibonacci (c) Thue-Morse (d) Rudin-Shapiro array. All the particles in the arrays have a radius of 100nm and a minimum separation of 25nm. (e) Scaling of the calculated intensity enhancement for the different arrays as a function of the number of particles.

The size dependent nature of the optical response of aperiodic systems is a direct manifestation of multiple scattering in the mesoscopic regime. On the other hand, no photonic coupling occurs in subwavelength packed periodic array, as evidenced by the strongly reduced phase modulation across the array plane in Fig. 3(a), and more delocalized plasmonic modes are formed across the entire periodic structure with reduced hot spot intensity. The lack of photonic-type coupling in closely packed periodic arrays prevents the onset of size-dependent photonic-plasmonic resonances and the resulting field enhancement effects, making the maximum hot spot intensity almost insensitive to the overall periodic array size, as shown in Fig. 3(e).
We conclude by noticing that the mesoscopic regime of aperiodic plasmon arrays has direct implications for optical device engineering. In fact, in addition to the particles composition/morphology and array geometry, we have demonstrated that the size of aperiodic arrays can be tailored in order to largely enhance the near-field hot spots intensity.

Nanofabrication of aperiodic nanostructures

In contrast to random media, DANS can be specifically tailored and fabricated using conventional nanolithographic techniques such as electron beam lithography (EBL) or Focused Ion Beam (FIB) milling followed by standard metal deposition and etching steps. Within this project, our group has recently developed a flexible process flow, sketched below, for the nanofabrication of arbitrary arrays of metal nanoparticles of interest to nanoplasmonic applications. Moreover, high-throughput fabrication was demonstrated recently by Lin et al. [29] who combined this approach with a reusable transfer imprint technique. Aperiodic nanoparticle arrays based on noble metals, typically Au and Ag, are

typically fabricated on quartz substrates using a 10 nm layer Indium Tin Oxide (ITO) to provide conduction.

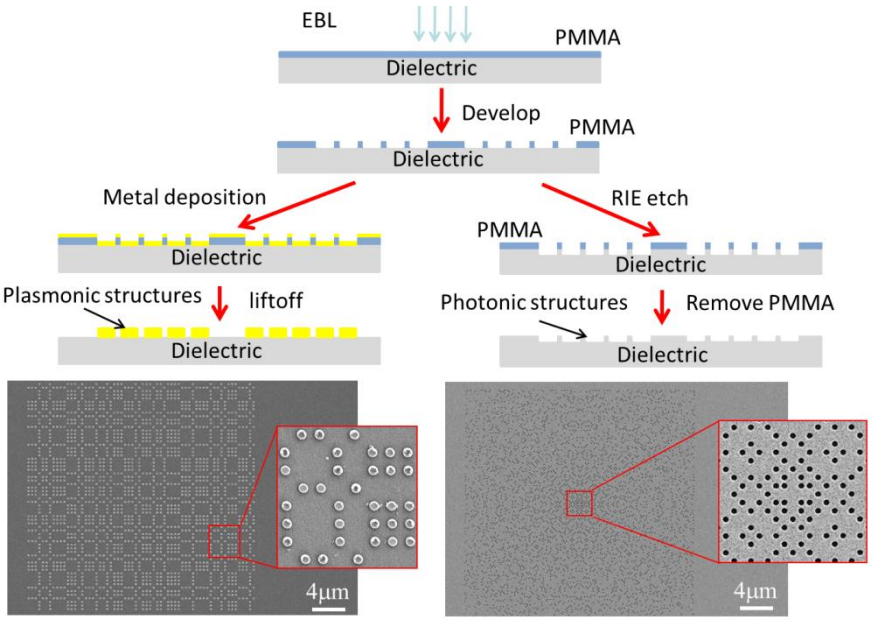

Fig. 4. Schematics of the fabrication process flow for the generation of aperiodic plasmonic nanoparticle arrays (left) and nano-hole arrays (right). The SEM pictures show a Rudin-Shapiro arrays of Au nanoparticles (left) and a Gaussian prime array of nano-holes in a quartz substrate. The particle/hole radius is 100nm and the minimum interparticle separation is 200nm.

A 180-nm-thick layer of PMMA (PolyMethylMethAcrylate) is then spin coated on top of the cleaned substrate. Subsequently, the DANS patterns are defined using a Zeiss SUPRA 40VP SEM equipped with a Raith Beam Blanker and NPGS for nanopatterning. After developing the resist in a 1:3 solution of MIBK (Methyl IsoButyle Ketone) and IPA (Isopropanol), a ~ 30nm thick Au/Ag film is deposited on the patterned surface by electron-beam evaporation. Finally, a liftoff process is performed using acetone, resulting in the definition of the targeted metal nanoparticle arrays.

Within the same general process flow, nano-perforated metal/dielectric films can also be obtained using by a Reactive Ion Etching (RIE) step immediately after the EBL writing. The process flow for the fabrication of both metallic nanoparticle arrays and nano-hole patterns is illustrated in Fig. 4. Typical dimensions of each fabricated array are about 100μm x 100μm for nanoparticles with a diameter of 200nm, 30nm tall and variable separations that can range in between 25nm and 400nm, depending on the specific DANS geometry, device applications, and nanolithographic setup.

As an example of fabricated DANS, we show in Figure 5 the Scanning Electron Microscopy (SEM) pictures of arrays of Au nanoparticles arranged in Fibonacci (a), Thue-Morse (b), Rudin-Shapiro (c), and co-prime (d) pattern geometries. The Au particles are cylindrical in shape and their height, as characterized by Atomic Force Microscopy (AFM) and SEM, was found to be h=30nm. All the particles have a circular diameter of d=200nm and a minimum interparticle separation a=25nm. Notice however, that additional length scales are present in aperiodic structures, extending to dimensions comparable to the wavelength of light in the optical regime.

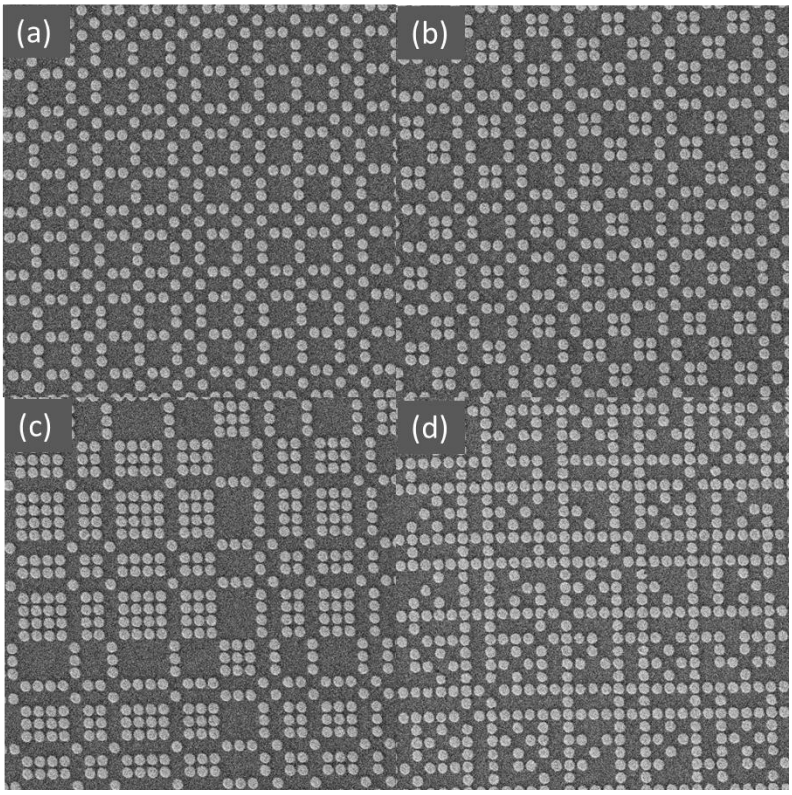

Fig. 5. SEM pictures of (a) Fibonacci, (b) Thue-Morse, (c) Rudin-Shapiro, (d) Coprime Au nanoparticle array. The individual particle sizes are 150nm, and the minimum interparticle separations in the arrays shown are 25nm.

To demonstrate the flexibility of the DANS fabrication approach described above, we show in Fig. 6 additional examples of Au nanoparticle arrays fabricated with various types of deterministic aperiodic order on Si substrates. These structures are a Danzer (a), Pinwheel (b), body-centered Pinwheel (c) and the three most investigated types of Vogel spiral arrays, namely the α_1-spiral (d), the golden angle spiral (e) and the α_2-spiral (f). We can clearly appreciate from Figures 5 and 6 the quality of the nanofabricated arrays, which excellently match the designed geometrical patterns over large device areas. *However, current nanoscale writing techniques, such as EBL, focused ion beam lithography (FIB), and scanning probe microscopy (SPM), suffer from high operating costs and low throughput.* In order to efficiently scale the dimensions of aperiodic plasmonic arrays to larger sizes in a cost-effective manner, novel fabrication methods are currently investigated. We notice that shadow-mask patterning techniques, such as stencil-based methods, allow for the large-scale fabrication of plasmonic nanostructures but inherently suffer from edge blurring and cannot produce plasmonic films perforated with nano-holes, which play an important role in nanoplasmonics.

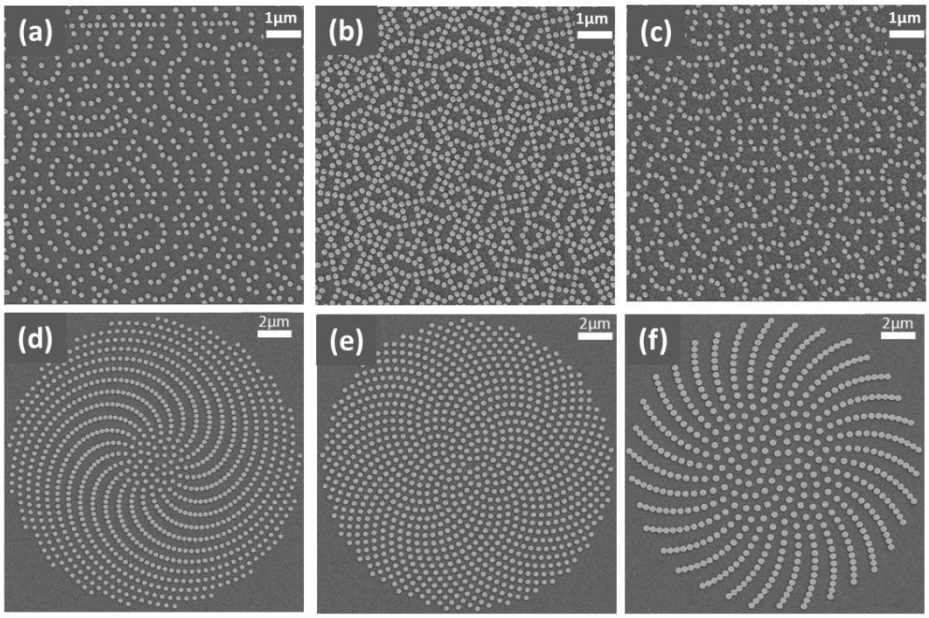

Fig. 6. SEM pictures of (a) Danzer, (b) Peenwheel, (c) Body centered pinwheel, (d) a_1 Spiral (137.3°), (e) golden Angle Spiral, (f) a_2 Spiral (137.6°) Au nanoparticle array. The individual particle sizes are 200nm, and the minimum interparticle separations in the arrays shown are 50nm.

To solve these problems, we have demonstrated a scalable and cost-effective direct transfer nanofabrication technique that utilizes a hard mold master and an inexpensive, commercially available flip-chip bonder, for the fabrication of large-scale metallic nanoparticles on polymer substrates and perforated metallic membranes (nano-hole arrays) atop silk fibroin films [29].

The process flow for the transfer imprint of plasmonic nano-dots and nano-holes, begins with the fabrication of the reusable master molds. We illustrate in Fig. 7 the successful printing of nano-dots on silk fibroins substrates and nano-hole arrays on a metal film. In the case of the nano-dot transfer process (Fig. 7a-d), the desired geometry is fabricated into a Si mold consisting of nanopillar arrays, while the nano-hole process requires a mold containing nano-holes, as shown in Fig. 7 (e-h). The fabrication of the nano-hole master proceeds via EBL writing with a 260nm-deep RIE step, using the PMMA as an etch mask. The remaining PMMA is removed by hot acetone bath, resulting in the Si nano-hole master. The Si master is first treated with a silanizing agent to reduce the adhesion of the Au to the Si surface. This surface treatment enables a higher yield in pattern transfer of the Au to the silk film in the subsequent steps. The process flow continues with the deposition of a 35nm-thick e-beam evaporated gold (Au) film, as shown in Fig. 7 (f).

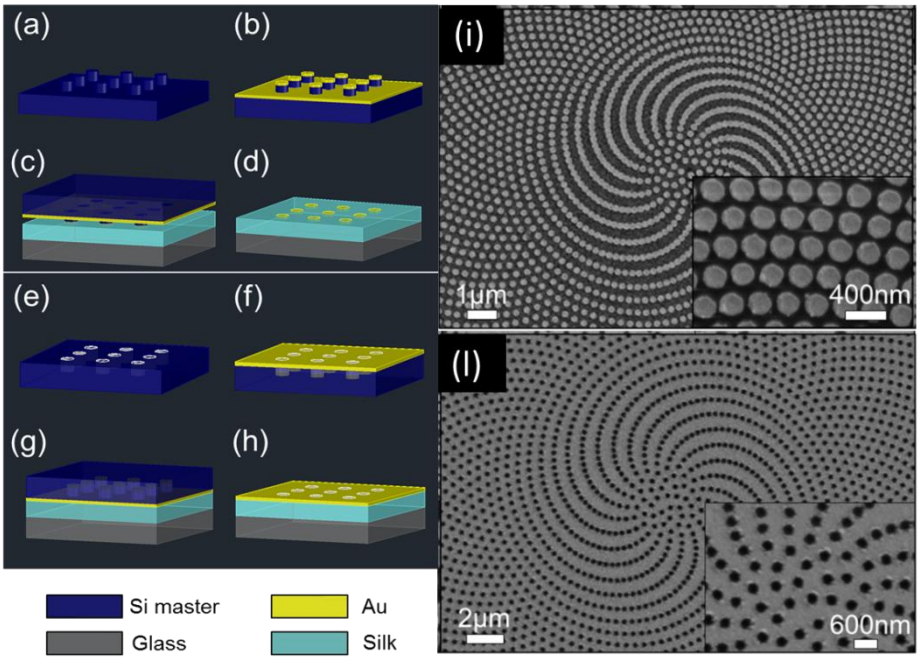

Fig. 7. Process flow of transfer nanoimprint of plasmonic nano-dots (a-d) and nano-hole arrays (e-h) using reusable masters. (i) Transferred plasmonic α_1 spiral nanodot array on silk film from Si master. (l) Transferred plasmonic α_1 spiral nano-hole array on silk film from Si master.

The Au coated master is now ready for transfer imprinting the plasmon membrane on the silk substrate (Fig. 7g-h). A commercial flip-chip bonder (Smart Equipment Technology FC150) was employed to transfer imprint from the fabricated master mold. The flip-chip bonder is used to align and bond one or more chips onto a substrate using pressure and heat. The transfer imprint process begins by heating the Au covered master to 90^{o}C, when it is then pressed onto the surface of the silk layer with a force of 50kg (area of 16mm^2) for 5min. During the imprinting, the plasmonic nanostructures bind to the surface of silk layer. Upon completion of the bonding cycle, the master is removed, leaving the Au embedded on the surface of the silk layer as shown in Fig. 7(h) for the case on nano-perforated membranes. Nano-imprinted plasmonic hole arrays with a representative Vogel spiral geometry [8] are shown as an example in Fig. 7 (l). A similar process has been successfully developed to imprint arrays of metallic nano-dots atop polymer films. In this case, a Si mold consisting of nanopillar arrays needs to be utilized, as illustrated in Figs. 7(a-d). The nanodot master fabrication proceeds with the deposition of 35nm-thick chrome (Cr) layer via electron beam (e-beam) evaporation, followed by a lift-off process in heated acetone. The resulting Cr nanocylinders serve as a etch mask for a 230nm-deep anisotropic reactive ion etch (RIE), forming the desired nanopillar array. The residual Cr layer is then removed by wet chemical etch. More details on these novel high throughput and scalable fabrication processes can be found in Ref [29].

Reusable transfer imprint enables large-scale replication of arbitrarily complex nanostructures with deep sub-wavelength details down to 30nm with a high throughput. The inexpensive scalability of aperiodic nanoplasmonic structures over large areas is of great importance for device engineering as it offers the opportunity to greatly reduce

fabrication costs and to develop aperiodic substrates into a mature technology for cost-effective device applications.

Light emission enhancement

We designed and fabricated Au nanoparticle arrays with quasi-periodic (Fibonacci) order and coupled them to light emitting Er-doped silicon nitride materials in order to investigate plasmon enhancement of 1.55 microns radiation [2].

A 3.6 times enhancement of the photoluminescence (PL) intensity accompanied by a reduction of the Er^{3+} emission lifetime at 1.54μm (see Fig. 8) has been observed and explained by the coupling of light emission with the broadband near-infrared structural resonances supported by the Fibonacci structure. Photonic-plasmonic hybrid Fibonacci modes were identified in a comparative transmission experiment between periodic plasmonic gratings and Fibonacci quasi-periodic structures by the spectral positions of transmission minima, in a large range of fabricated structures. The scaling behavior of the emission enhancement in Fibonacci and periodic gratings was discussed in relation to the modifications of the photonic Local Density of States (LDOS) at the Er emission wavelength. The strongly reduced frequency sensitivity of the photonic-plasmonic scattering resonances in Fibonacci arrays prevented the detuning from the Er emission wavelength, and increased Er emission across its entire spectrum.

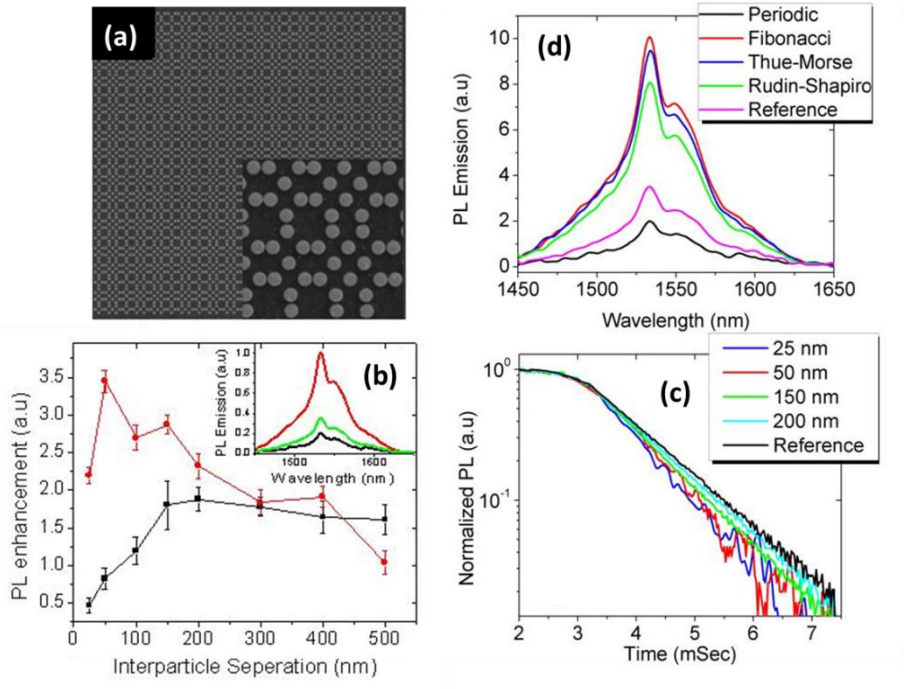

Fig. 8. Demonstration of light emission enhancement from Erbium atoms coupled to deterministic aperiodic plasmonic arrays of Au nanoparticles (200nm diameter) (a) SEM picture of quasiperiodic Fibonacci Au nanoparticle array fabricated atop a light emitting Er:SiN_x substrates of 80nm thickness. (b) Integrated PL enhancement in periodic (black) and Fibonacci (red) arrays of various interparticle separations. The inset shows representative PL spectra of periodic (black), Fibonacci (red) arrays and of the unpatterned (green) region. (c) PL decay time of Er atoms through unpatterned substrate (black) and Fibonacci arrays with varying interparticle separations indicated in the legend. (d) PL spectra excited at 488nm of periodic and aperiodic nanoparticle arrays (50nm min interparticle separation).

Moreover, when decreasing the interparticle separation in the Fibonacci arrays, the emission intensity was found to increase along with the emission rate, while an opposite behavior, indicative of non-radiative losses, was observed in periodic grating structures. The coupling of light emission to the broadband scattering resonances of quasi-periodic Fibonacci arrays makes these systems particularly attractive for radiative rate engineering applications that require light extraction/enhancement over broad frequency spectra.
We also developed an alternative approach to light emission enhancement based on the engineering of circular light scattering in plasmonic Vogel's spirals [8]. We demonstrated that this can result in broadband light emission enhancement in active thin films coupled to deterministic aperiodic structures. Within this project we have investigated the impact of the inhomogeneous distribution of local spatial frequencies of Vogel spirals on their emission patters. In particular, we prepared a dye polymer solution by dissolving common laser dye molecules of DCM (Exciton Inc.), in toluene.

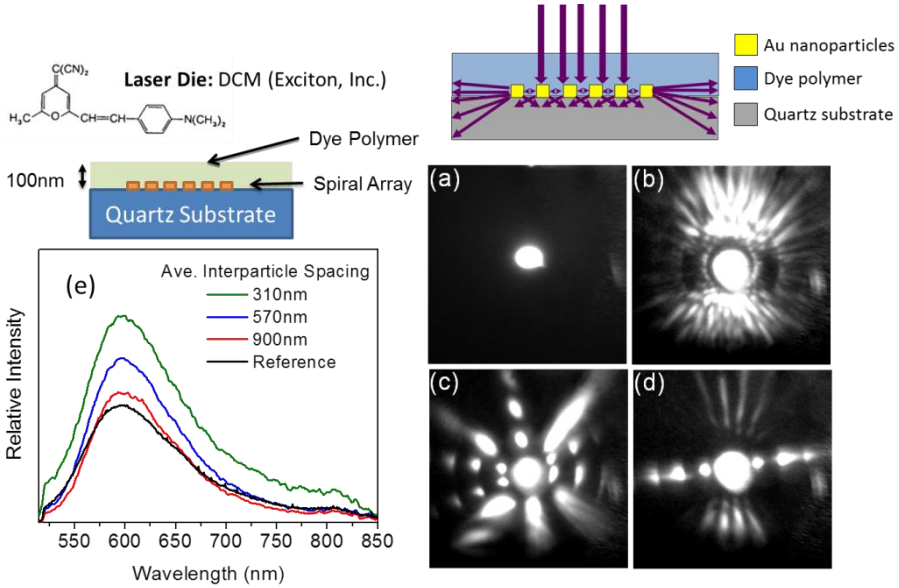

Fig. 9. (top) Schematic cross-section of Au spiral nanoparticle array on a quartz substrate, coated with DCM doped PMMA. Nanoparticles are cylindrical in shape with 200nm diameter and 30nm in thickness with array diameter of 100μm. (a-d) CCD images of light emission from a DCM dye layer (100nm thick) deposited onto: (a) homogeneous quartz substrate (b) dye emission from scattered light of α_2-spiral (27,778 particles) with laser positioned at the center of the spiral. (c) and (d) dye emission from scattered light of α_2-spiral with laser positioned off center of the spiral. (e) Photoluminescence spectra of doped polymer form samples coupled to α_2-spiral arrays with varying average interparticle separations (310nm, 570nm, 900nm and un-coupled film for reference).

The dilute solution was then mixed with Polymethylmethacrylate (PMMA), spun onto samples and cured, resulting in 100nm thick films of laser dye doped PMMA. This particular laser dye has maximum absorption at 480nm and an emission peak at 640nm, which overlaps the scattering resonances of the investigated α_2-spiral, leading to broadband emission enhancement, shown in Fig. 9. Moreover, we demonstrate the ability to dramatically modify the angular emission of the sample by imaging the fluorescence in

transmission under for different excitation conditions (Figs. 9a-d). In particular, the sample was pumped by positioning the laser spot at different locations onto the doped PMMA substrate at normal incidence (focused through a 10x objective) with a laser diode at 480nm and the emitted light was collected in transmission configuration through the substrate using a lens of 100mm focal length, and imaged by a CCD camera. In order to capture only the emission patterns, the pump laser light was blocked by a 514nm high-pass filter. An identically prepared emitting layer was also coated on unpatterned quartz for reference. Figure 9 (a) shows the CCD image of the fluorescence collected in transmission through the reference sample (i.e., with no spiral pattern), which indicates that the fluorescence is spatially confined to the pumped region in the absence of scattering structures. On the other hand, when pumping the samples with the plasmonic arrays, the fluorescence spreads laterally in the plane of the array and, when the sample is symmetrically pumped through its center, a significant fraction of the fluorescence is emitted along multiple directions due to the isotropic character of the Fourier space (i.e., circular light scattering), as demonstrated in Figs. 9 (b). Moreover, when the position of the laser pumping spot is slightly misplaced from the center of the sample (in the horizontal direction) by approximately 25μm, the angular distribution of the radiation changes dramatically due to the very inhomogeneous distribution of local spatial frequencies associated to the surface of aperiodic spirals with circularly-symmetric Fourier space, as shown in Figs. 9(c-d). These results demonstrate that aperiodic arrays with Vogel spiral geometry can be utilized to enhance and manipulate light emission in planar structures. While more work is required to fully leverage aperiodic spiral order for active optical devices, we believe that this work motivates the development of novel optical devices for polarization insensitive, enhanced light-matter coupling on planar surfaces, such as plasmonic photodetectors and thin-film solar cells, which will be briefly reviewed next.

Thin-film solar and photodetectors enhancement

In order to broaden the spectral region of light absorption enhancement, it is crucial to engineer aperiodic nanoparticle arrays with a higher density of spatial frequencies and a high degree of rotational symmetry without resorting to uncontrollable random systems, which have only limited engineering appeal. Recent studies have proposed to utilize plasmonic arrays with aperiodic quasicrystal structures, such as Penrose lattices, which exhibit non-crystallographic rotational symmetries. Such arrays, by virtue of their higher degree of rotational symmetry compared to traditional periodic structures, give rise to enhanced scattering along multiple directions and over a broader wavelength range, producing coherent wave interactions among an increased number of neighboring particles. There is currently the need to engineer densely-packed arrays of nanoparticles/nano-holes with continuous circular symmetry providing polarization isotropy and efficient planar light diffraction within targeted spectral ranges. In addition, such effects should occur regardless of the direction of incident radiation, thus eliminating the need to costly tracking schemes in solar cells applications.

In this project, we have recently proposed and utilized plasmonic aperiodic Vogel spiral arrays as a viable strategy to achieve wide-angle light scattering for broadband and polarization insensitive absorption enhancement in thin-film Si solar cells [22]. Our group has previously demonstrated that aperiodic Vogel spiral arrays feature nearly

continuous azimuthal symmetry in Fourier space [8,18,25] and, when normally illuminated, satisfy the Rayleigh condition for planar light scattering over broad and controllable frequency bands, irrespective of the incident polarization of light. A simple scalar Fourier optics picture already suggests that polarization-insensitive large-angle scattering of incident radiation occurs in GA spiral arrays at frequencies matching the radial position of the scattering ring in reciprocal space. This property is ideal to manipulate light trapping in thin-film Si solar cells. Following this approach, we designed and fabricated GA arrays of Au nanoparticles atop ultra-thin film (i.e., 50nm-thick absorbing amorphous Si layer) Silicon On Insulator (SOI) Schottky photodetector structure, as sketched in Fig. 10, and we demonstrated experimentally larger photocurrent enhancement in the 600nm-950nm spectral range compared to optimized nanoparticle gratings. The relation between the spatial Fourier spectrum of GA arrays of Au nanoparticles and the large angular distribution of scattered radiation in the forward scattering hemisphere has been rigorously investigated by calculating the angular radiation diagrams using the Coupled Dipole Approximation (CDA) methods for particles with ellipsoidal shape.

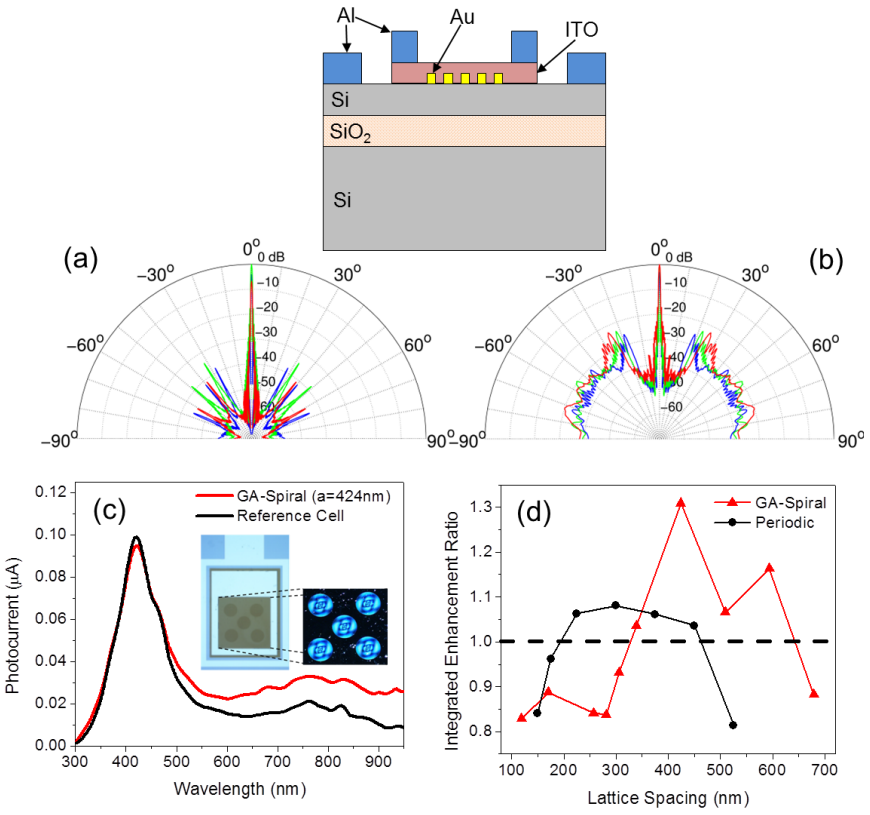

Fig. 10. (top) Schematics of the device cross-section of the SOI Schottky photo-detector with plasmonic arrays integrated onto the absorbing surface. (a,b) Calculated radiation diagrams as a function of the inclination angle for a GA spiral (a) and a periodic array (b) for three different wavelengths, namely 480nm (Blue), 520nm (Green), and 650nm (Red). (c) Spiral array photocurrent with average center to center spacing of 425nm (red) and empty neighbor references cells (black). (d) Integrated photocurrent enhancement ratio for GA spiral (red) and periodic (black dashed) arrays of different center to center particle spacing.

This CDA approach is particularly suited to efficiently treat large-scale plasmonic systems of small and well-separated nanoparticles, and it has been previously validated against semi-analytical multiple scattering methods. In our work, all nanoparticles were modeled by oblate spheroids with 100nm diameter and 30nm height. Moreover, the arrays are embedded in Si and normally excited by a linearly polarized plane wave. The parameter of interest for the understanding of the angular scattering properties is the differential scattering cross section, which describes the angular distribution of electromagnetic power density scattered at a given wavelength within a unit solid angle centered around an angular direction (θ,φ) per unit incident irradiance. In the case of arrays composed of dispersive metal nanoparticles, the power scattered from a particular structure is generally a function of both the geometrical parameters of the array and the wavelength of the incident radiation. Full information on angular scattering is thus captured by calculating the averaged differential scattering cross section, where the average is performed on the azimuthal angle φ and the scattered intensity is normalized to the maximum value (i.e., forward scattering peak). By plotting the azimuthally averaged differential scattering cross section versus the inclination angle, we obtain the radiation diagrams of the arrays. In Figs. 10(a,b) we show (plotted in dB scale) the calculated radiation diagrams for a periodic grating structure and the optimized GA arrays at three different wavelengths λ_B=480nm, λ_G=550nm and λ_R=610nm (i.e corresponding to the blue, green, and red colors), respectively. Differently from the well-known case of periodic structures, where the scattered radiation is preferentially redistributed along the directions of coherent Bragg scattering (Fig. 10a), the radiation diagram of GA arrays is significantly broadened at large angles (i.e. >30°) for all the investigated wavelengths, demonstrating broadband wide-angle scattering behavior (Fig. 10b).

By combining experimental absorption enhancement and photocurrent measurements with CDA and full-vector 3D Finite Difference Time Domain (FDTD) simulations, we recently demonstrated that broadband wide-angle scattering in GA spiral arrays redirects a larger fraction of the incident radiation into the absorbing Si substrate. Moreover, this effect increases the optical path of photons in the photodetector, as well as enhancing the coupling to LSPs in the array plane. In Fig. 10(c) we show the measured photocurrent spectra for the best performing GA spiral photodetector device. The reference line shows the photocurrent spectra measured on the unpatterned devices in the nearest reference cells, respectively. A maximum photocurrent enhancement of approximately a factor of 3 is measured for the GA spiral at 950nm. Such an increase in photocurrent results from the interplay of plasmonic-photonic coupling in GA spirals, which contribute to the overall enhancement as follows: by providing more efficient coupling of incident radiation into the thin Si layer due to photonic wide-angle scattering; by enhancing the intensity of the near-fields around the nanoparticles at the Si interface owing to better LSP coupling in the plane of the array compared to periodic structures. A detailed comparison with optimized periodic grating structures in discussed in Ref. [22].

In Fig. 10(d) we show the integrated photocurrent enhancement ratio, calculated by the ratio of the integrated photocurrent spectrum of the device with and without plasmonic arrays. The ratios falling below the dotted line indicate devices with overall reduced performance when compared against their neighboring empty reference cells. We see in Fig. 10(d) that both GA spiral and periodic arrays exhibit an optimization trend with respect to the interparticle spacing, yielding maximum integrated enhancements of 8%

and 31% over the reference cells, respectively. We observe finally that the experimentally measured 31% integrated enhancement of GA spiral arrays has been demonstrated covering only 25% of the active photodetector area by GA arrays (Fig 10c, inset).
The significant photocurrent enhancement values demonstrated for devices coupled to GA spirals highlight the potential for even greater performances in the case of complete coverage of the device area.

Spatial-spectral detection with colorimetric fingerprints

In this project we have developed a novel concept for optical biosensing based on the engineering of colorimetric fingerprints in aperiodically nanopatterned surfaces [4,5]. Light scattered from these surfaces is localized in different areas of the devices and gives rise to complex color structures that specifically fingerprint the aperiodic surface.
In current biosensing technology, two-dimensional optical gratings provide a well-established platform for biochemical colorimetric detection and enabled label-free sensing of various molecular analytes and protein dynamics. Periodic grating biosensors provide a distinct change in the intensity of diffracted light or in the frequency spectrum of optical resonances in response to variations of refractive index. The physical mechanism at the basis of the colorimetric response is the well-known phenomenon of *Bragg scattering*. While this process provides frequency selective responses that are useful for colorimetric detection, the ability of light waves to interact with adsorbed or chemically bound analytes present on the surface of the sensors is intrinsically limited. In fact, Bragg scattering is a first-order process in surface scattering perturbation theory, and scattered photons easily escape from a periodic surface without prolonged interaction with the sensing layer. On the other hand, engineering multiple light scattering in planar aperiodic structures provides novel opportunities for bio-chemical sensing applications because it enables much longer photon dwelling times with the sensing areas. In particular, optical sensing platforms can be boosted by developing scattering elements that simultaneously provide high sensitivity to the environmental changes and high spectral resolution, as both factors contribute to the improvement on the sensor detection limit. Detector sensitivity is conventionally defined as the magnitude of the wavelength shift induced by a change in the ambient refractive index (measured in nm/RIU), and can be improved by enhancing light-matter interactions on a planar substrate. In turn, the resolution in measuring wavelength shifts inversely depends on the linewidth of the resonant mode supported by the structure. We have demonstrated that aperiodic photonic structures provide the necessary balance between the resonant character of their resonant modes and the spatial distribution of large field intensity over extended sensing areas, resulting in largely improved sensitivity over periodic grating sensors and or photonic crystals cavities, which are limited by the small overlap of the analyte with the localized field. Building on these results, we have introduced within this prpoject a novel approach to label-free optical biosensing based on micro-spectroscopy and spatial correlation analysis of structural color patterns excited by white light illumination in DANS metal-dielectric surfaces [4]. In contrast to traditional photonic gratings or photonic crystals sensors (which efficiently trap light within small-volumes), aperiodic scattering sensors sustain distinctive resonances localized over larger surface areas.

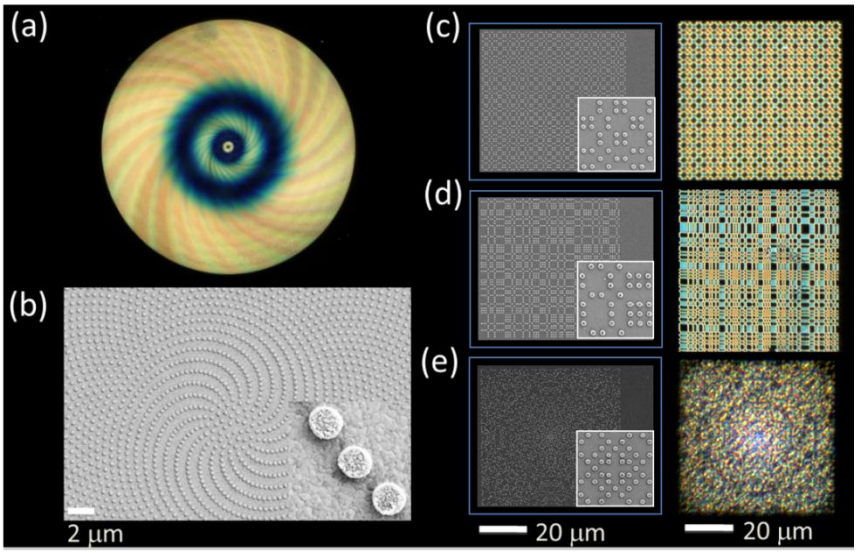

Fig. 11. (a,b) Colorimetric fingerprint of as α_2 aperiodic spiral array of Al nanoparticles measured by dark-field microscopy and an SEM picture (b) showing a detail of the structure. SEM pictures of (a) Fibonacci array, (d) Rudin-Shapiro array, and (e) Gaussian prime array of Au nano-cylinders with radius r=100nm, height h=30nm, and minimum interparticle separation d=25nm. The color figures in (c-e) are the corresponding "colorimetric fingerprints" measured by dark-field microscopy under white light illumination.

These structural resonances, known as *critical modes*, are described by highly fluctuating field profiles described by multi-fractal analysis and possess a dense spectrum, resulting in efficient photon trapping through higher-order multiple scattering processes on the surface of the devices. These distinctive scattering behavior strongly enhance the sensitivity of DANS surfaces to small refractive index variations. The complex spatial patterns of critical modes offer the potential to engineer structural color sensing using spatially localized patterns at multiple wavelengths. In fact, when illuminated by white light, DANS surfaces feature highly structured multi-color scattering patterns which are a sensitive fingerprints of the aperiodic geometries, known as *colorimetric fingerprints*. When light is incident on aperiodic surfaces with engineered geometry and particle separation, distinct optical frequencies (i.e., colors) localize in different areas of the device and can readily be observed in the object-plane or in the far-zone, as demonstrated by the color patterns in Fig. 11. Adding a thin layer of analyte on top of aperiodic arrays shifts the resonance wavelengths of the resonances supported by the aperiodic surface leading to a spatial rearrangement of the localized field intensity across the area. Due to the critical nature of the resonant states, which are spatially extended though highly fluctuating in space, a global change in the colorimetric pattern of scattered radiation can readily be detected.

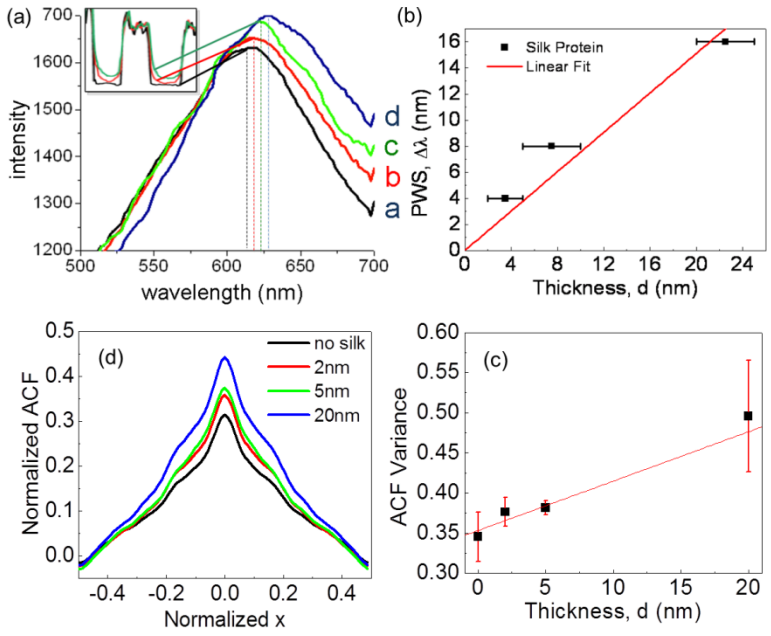

Fig. 12. (a) Coating of different thicknesses of silk protein monolayers were characterized by Atomic Force Microscopy (insert) and the colorimetric responses of the associated arrays were measured spectrally. Coating of different thicknesses of silk protein monolayers were characterized by Atomic Force Microscopy (insert) and the colorimetric responses of the associated arrays were measured spectrally. (b) The sensitivity of the arrays is quantified by the spectral shift of the scattered radiation peaks (PWS) per thickness variation of the protein layer. (d) 1-D ACF profiles extracted from 2-D normalized autocorrelation function along the x-axis of the middle of the images. (c) The changes of patterns due to different thicknesses of silk protein monolayers are quantified by the normalized ACF variances.

The colorimetric fingerprints of nano-patterned deterministic aperiodic surfaces occur over a broad spectral-angular range and can be captured using conventional dark-field microscopy, as demonstrated in Fig. 11. As a result, engineered colorimetric fingerprints of aperiodic surfaces can be used as a transduction mechanism in a novel type of highly sensitive label-free multiplexed sensor. In such sensing device, both the peak wavelength shifts (Fig. 12a,b) of scattered radiation as well as the environment-dependent spatial structure of the colorimetric fingerprints (Fig. 12 c-d) can be utilized to detect the presence of nanoscale protein layers on the surface of DANS. The proposed approach is intrinsically more sensitive to local refractive index modifications compared to traditional ones due to the enhancement of small phase variations, which results from the multiple scattering regime.

The spatial modifications of the structural color fingerprints induced by small refractive index variations can be quantified using standard image autocorrelation analysis performed directly on the scattered radiation. This can be accomplished in two modalities: (a) using polychromatic or (b) single wavelength radiation, as shown in Fig. 12 in the case of silk protein monolayers deposited on engineered DANS surfaces. To construct the image autocorrelation function, the value of the field intensity at point (x, y) in the array plane is compared with that at another point (x', y') and mapped as a function of the distance between the two points. 1D profiles through the 2D autocorrelation function of the intensity images in Fig. 12(d). The initial decay in the ACF reflects local short-range correlations in the aperiodic structure, and any long-range periodicities in the

intensity pattern give rise to periodic oscillations in the ACF. To quantify the overall change in the colorimetric pattern induced by the presence of thin molecule layers, we calculate the variance of the fluctuations in the intensity distribution function, which can be found as the value of the properly normalized discrete ACF in the limit of zero lateral displacements. The proposed approach recently led to the demonstration of femto-molar detection of silk proteins adsorbed on DANS.

The refractive index modifications induced by the analytes (silk protein) can be detected by frequency shifts *and* a global structural color modification. Combining Electron Beam Lithography (EBL), dark-field scattering micro-spectroscopy, autocorrelation analysis and rigorous multiple scattering calculations based on the Generalized Mie Theory (GMT). *In this project we have engineered aperiodic arrays of metal nano-particles on quartz substrates, and showed that the information encoded in both the spectral and spatial distribution of structural resonances can be simultaneously utilized for sensitive bio-detection on the nanoscale [4,5,28]*. The potential of the proposed approach for rapid, label-free detection and recognition of biomolecular analytes in the visible spectral range was experimentally demonstrated by the distinct variation in the spectral and spatial colorimetric fingerprints in response to monolayer increments of protein layers sequentially deposited on the surface of aperiodic arrays of nanoparticles.

Recently, we also demonstrated successful integration of aperiodic arrays of metal nanoparticles with microfluidics technology for optical sensing using the spectral-colorimetric responses of the nanostructured arrays to refractive index variations (S.Y. Lee et al., in review). In particular, they fabricated different aperiodic arrays of Au nanoparticles with varying interparticle separations and Fourier spectral properties using Electron Beam Lithography (EBL) and integrated them with polydimethylsiloxane (PDMS) microfluidics structures by soft-lithographic micro-imprint techniques.

The fabrication process flow that enabled the optofluidic integration of DANS is schematically illustrated in Fig. 13 (a). In our integration process, a 28μm-thick SU8 negative photoresist, with an additional 1μm-thick SU8 filling groove for facilitating fluid filling into microchannels, was first spin-coated on a cleaned silicon wafer and microfluidic structures were defined on the substrate through standard photolithography. A thin layer of PDMS (10:1 base: curing agent) was subsequently cured on top of the SU8 master at 70^{o}C for 2 hours. Half-through inlet and outlet holes were bored on the PDMS mold at both ends of the transferred microchannel patterns and the PDMS mold was oxygen-plasma treated along with the colorimetric DANS sensor on SiO_2 substrate to form an optofluidic DANS device.

The oxygen plasma process permanently bonded the device together and resulted in hydrophilic surfaces, which easily prime the microchannels with insensible amount of pressure. Epidermic syringe needles were then inserted from the sides of the PDMS mold into the holes as fluid access ports and secured using silicone sealant, as shown in Fig. 13 (b,c). Figure 13(b) clearly illustrates optofluidic DANS devices under a microscope, in which various types of arrays were positioned inside the microfluidic flow cell for colorimetric detection.

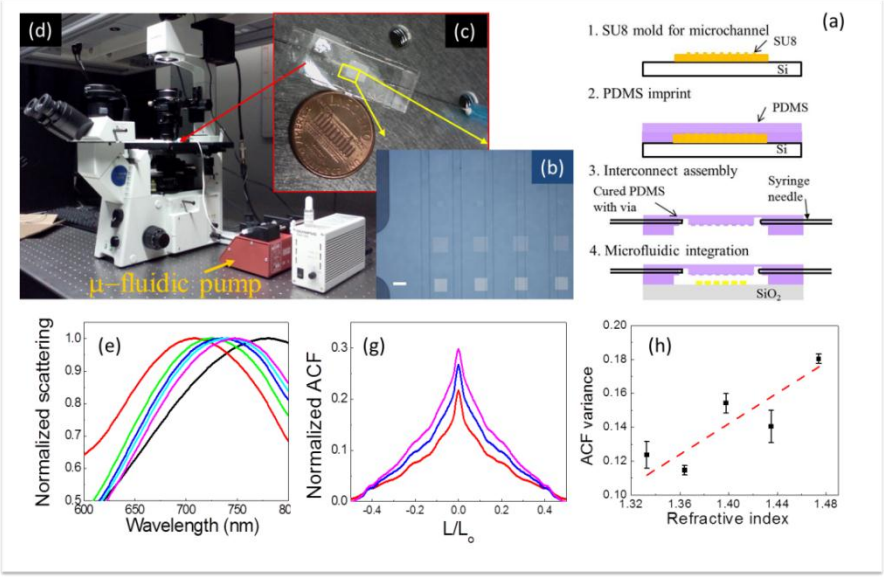

Fig. 13. (a) Fabrication process flow of PDMS micro-channel and microfluidic integration with colorimetric DANS sensing structures. (b) optical microscope image of the microfluidic flow cell with different 2D aperiodic arrays. The scale bar equals 100μm. (c) Digital image of a packaged optofluidic DANS device. (d) Dark-field microscope setup utilized for sensing characterization of fabricated devices. (e) Plasmon-enhanced linear scattering shift of microfluidics integrated DANS substrates. (g) Variation of autocorrelation functions of the scattered radiation from microfluidics integrated DANS sensors immersed in a liquid with varying refractive index. (h) Measured dependence of the autocorrelation functions of the scattered radiation in a microfluidics channel as a function of the liquid refractive index.

Spectral shifts of scattering spectra and the distinctive modifications of structural color patterns induced by refractive index variations were simultaneously measured inside microfluidic flow cells by dark-field spectroscopy and image correlation analysis in the visible spectral range, as demonstrated in Figs. 13 (e-h). The main outcome of this study is that aperiodic plasmonic Galois arrays result in large fluctuations of colorimetric fingerprints simultaneously accompanied by large wavelength shifts of their scattering spectra, providing both high spectral and colorimetric sensitivities within a microfluidic device. The integration of plasmonic aperiodic arrays with microfluidics devices provides a novel approach with multiplexed spatial-spectral responses for opto-fluidics platforms and lab-on-a-chip optical biosensing.

Engineering optical angular momentum of light with aperiodicity

During this project we have discovered that Vogel spiral nanoparticle arrays, when illuminated by optical beams, give rise to scattered radiation carrying OAM [8]. Dal Negro et al. [27] developed an analytical model that captured in closed form solution the Fourier and diffraction properties of arbitrary Vogel spiral arrays and demonstrated that light diffraction by Vogel spirals encode in the far-field OAM values arranged in aperiodic sequences associated to number-theoretic properties of the spirals. More precisely, the OAM values diffracted in the far-field are determined by the rational approximations, given by the continued fraction expansion, of the irrational divergence angles of Vogel spirals. In particular, wave diffraction by GA arrays encodes a Fibonacci sequence of OAM values in the Fraunhofer far field-region [27].

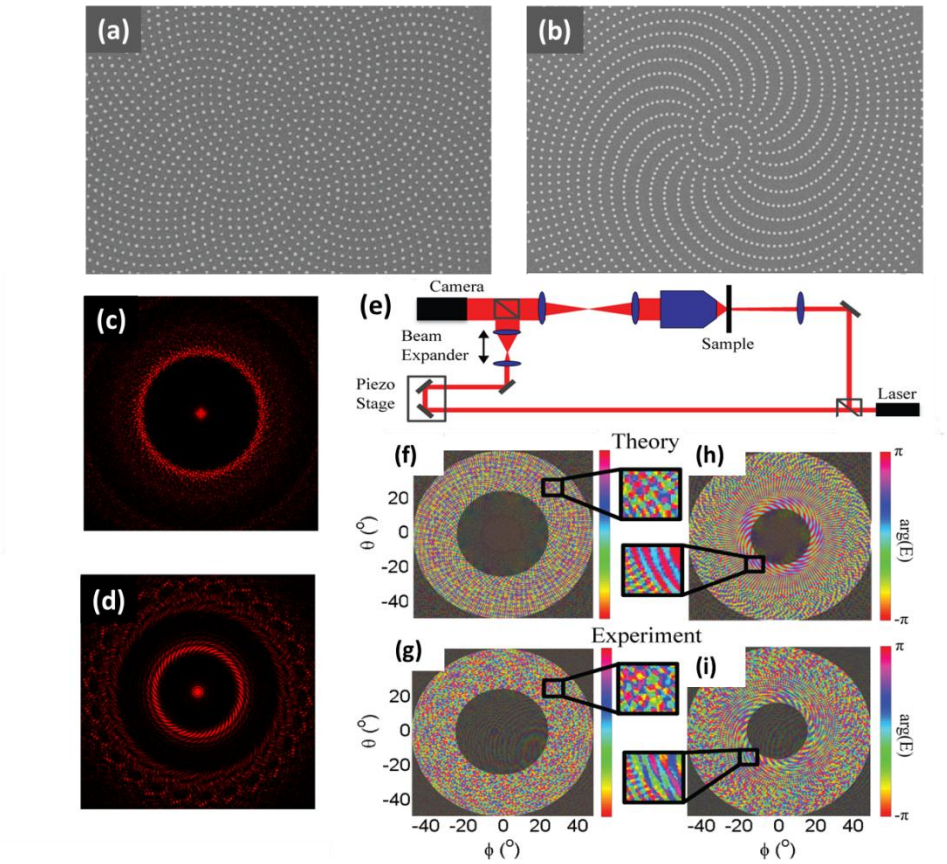

Fig. 14. (a,b) (a,d) SEMs of GA and μ spirals respectively composed of 500nm diameter gold nanoparticles on fused silica. (c,d) Analytically calculated far field intensity from the spirals in (a,b) at 633nm. (e) Optical set up used for the complex amplitude retrieval (f,h) Analytically calculated phase portrait of far field radiation from GA and μ spirals respectively. (g,i) Experimentally measured phase portrait from GA and μ spirals, respectively. Shaded areas indicate regions where the field intensity is too low to measure the phase accurately. These regions are ignored in the FHD.

Controlled generation and manipulation of OAM states with large values of azimuthal numbers has been recently demonstrated experimentally in this project by Lawrence et al. [31] using various types of Vogel arrays of metal nanoparticles. The OAM content of a diffracted optical wave at 633nm was analyzed using phase stepped interferometric measurements to recover the complex optical field. Fourier-Hankel modal decomposition of scattered radiation was performed to demonstrate the generation of OAM sequences from Vogel spirals. The samples consisted in arrays of Au nanoparticles fabricated on fused silica using electron beam lithography, metal evaporation and lift-off processing [31]. The SEMs of fabricated arrays are shown in Figs. 14(a,b). The corresponding far-field diffraction patterns are shown in Figs. 14 (c,d). In Fig. 14(e) we show the optical set-up used to measure the complex far field. A HeNe laser was weakly focused to a spot size of 50μm, from the rear of the sample and the scattered light from the array was collected by a 50X (NA=.75) objective. Two additional lenses were added to image the far field at the plane of the CCD[31].

In order to measure the phase of the far field radiation a reference beam was reflected from the piezo stage mounted mirrors, expanded and directed to the CCD. Multiple interference patterns were collected by increasing the piezo bias voltage, scanning the phase of the reference beam. A phase retrieval algorithm was finally used to recover the phase of the scattered light relative to the one of the reference beam. The analytically calculated phase of the far field radiation from GA and μ spirals is shown in Figs. 14(f,h) respectively. The measured phase from a GA spiral is shown in Fig. 14(g) and the phase from a μ spiral is shown in Fig. 22(i).

Modal decomposition was used to analyze a superposition of OAM carrying modes in the far field pattern and determine their relative contribution. Decomposition into a basis set with azimuthal dependence, is accomplished through Fourier-Hankel decomposition (FHD) according to [15,18,25,27,31]:

$$f(m,k_r)=\frac{1}{2\pi}\int_0^{\infty}\int_0^{2\pi} rdrd\theta E_{\infty}(r,\theta)J_m(k_r r)e^{im\theta}$$

where J_m is the m-th Bessel function. In this decomposition the m-th order function carries OAM with azimuthal number m, this can accommodate positive and negative integer values for m. Since we are primarily concerned with the azimuthal component of the field we can sum $f(m,k_r)$ over radial wavevectors k_r. In Figs. 15(a,b) the summed FHD of the calculated far field radiation from GA and μ spirals are shown, respectively. Both show peaks at azimuthal numbers corresponding to the denominators of the rational approximations (i.e., convergents) of the irrational divergence angles used to generate the spirals, as amply discussed in Ref. [27]. For the GA spiral this results in encoding the Fibonacci sequence in the OAM spectrum. The μ spiral has significantly fewer convergents in our region of interest, however some OAM peaks are observed at linear combinations of convergents. These peaks can be reduced with aperturing of the beam.

The values of OAM peaks can be explained based on the analytical far field radiation pattern theory developed by Dal Negro [27]. Here it suffices to remind that the FHD of the Vogel far field radiation pattern, is given by [27]:

$$f(m,k_r)=\sum_{n=1}^{N}A_m(k_r)e^{inm\alpha}$$

where, N is the number of particle in the array and $A_m(k_r)$ gives k_r dependent coefficients which we will ignore as we are primarily concerned with the azimuthal component. When $m\alpha$ is an integer, the N waves in the equation above will be in phase and produce an OAM peak at azimuthal number m. If α is an irrational number, this condition will never be satisfied. However, an irrational can be approximated by rational fractions (convergents) which make the product $m\alpha$ approximately an integer when m equals the different denominators of the convergents [27].

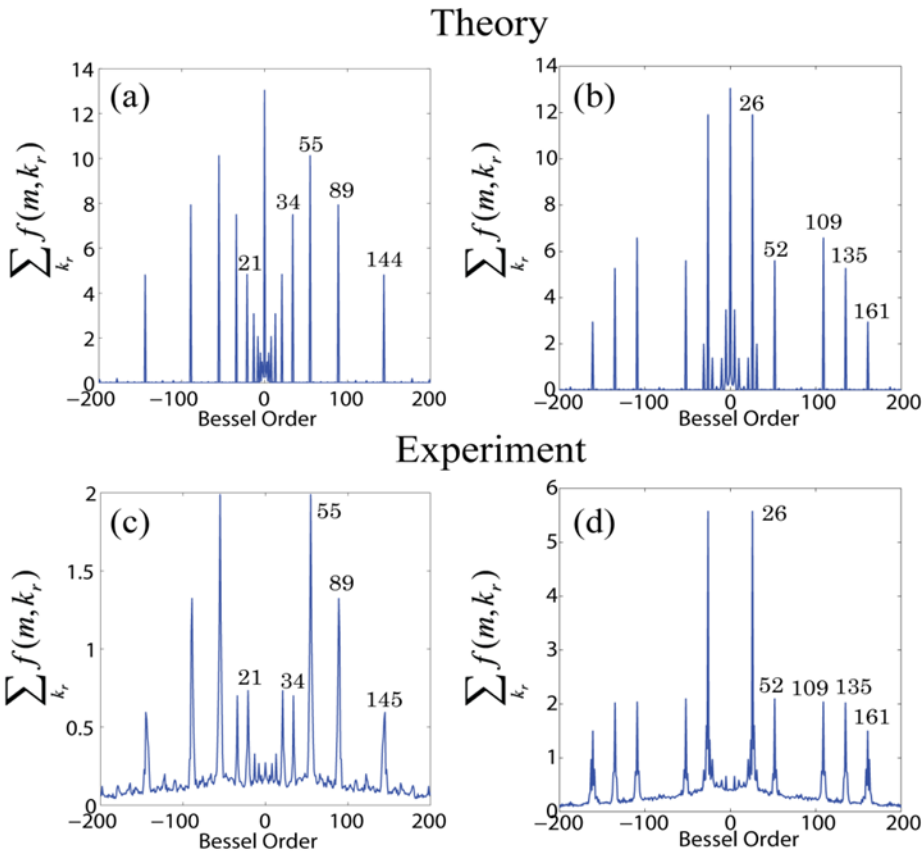

Fig. 15. Fourier-Hankel decomposition, summed over radial wavevector, for GA spirals (a,c) and μ spirals (b,d). In (a,b) FHD is obtained using analytically calculated far field, while in (c,d) FHD is obtained using experimentally measured far field.

This result was demonstrated by examining the OAM content of the experimentally measured scattered radiation. The reconstructed complex field (Figs. 14(g,i)), is decomposed into azimuthal and radial components. The shaded areas in Figs. 14(f-i) indicate the limits (angular range) where the measurement of the scattered light is accurate due to the limitations of the experimental setup. Figure 15 directly compares the predicted OAM spectra (i.e., radially summed FHD) and the experimentally measured ones. In Fig. 15(c) experimental results are shown for the GA spiral and peaks in the transform are observed at numbers corresponding to the Fibonacci sequence. In Fig. 15(d) peaks are observed matching the theoretically predicted values for the μ spiral. A full list of analytically calculated and the experimentally measured FHD peak positions can be found in Ref [31].

Finally, we have demonstrated direct excitation of optical modes carrying OAM values in light-emitting dielectric GA spiral structures consisting of Er-doped SiN nanopillars []. The successful demonstration of the superposition of many OAM modes in engineered Vogel spiral arrays of Au nanoparticles provides novel exciting opportunities for radiation engineering that are of interest to secure optical communication, classical, and quantum cryptography.

Deterministic aperiodic lasers

In this project we finally demonstrated, in collaboration with Yale University, the first laser action from a multiply scattering pseudo-random medium [7]. This is a breakthrough results in the field of complex lasers since we have experimentally demonstrated that deterministic aperiodic lasers behave similarly to random lasers but the frequency positions of their many lasing modes are completely predictable.

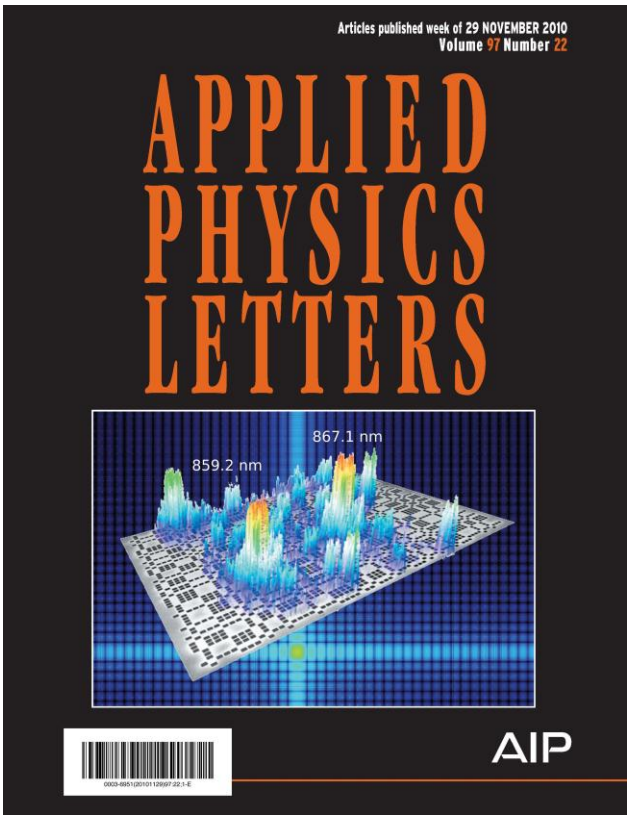

Fig. 16. Cover of Applied Physics Letters "*Demonstration of laser action in a pseudorandom medium*", 97, 223101 (2010)

We have demonstrated experimentally that the localized lasing modes in the Rudin-Shapiro arrays of air nano-holes in GaAs membranes occur at reproducible spatial locations and their frequencies are only slightly affected by the structural fluctuations in different samples. Numerical study on the resonances of the passive systems and optical imaging of lasing modes enabled us to interpret the observed lasing behavior in terms of distinctive localized resonances in the two-dimensional Rudin-Shapiro (RS) structures. Although the relatively narrow gain spectrum of InAs quantum wells does not allow broad-band lasing in the current samples, our numerical simulations confirmed that the RS structures support many localized modes of distinct frequencies. We expect lasing over a wide frequency range once switching to broad-band gain media such as semiconductor quantum dots. The deterministic aperiodic Rudin-Shapiro systems provides an alternative approach from random media and photonic crystals for the

engineering of multi-frequency coherent light sources and complex cavities amenable to predictive theories and technology integration.

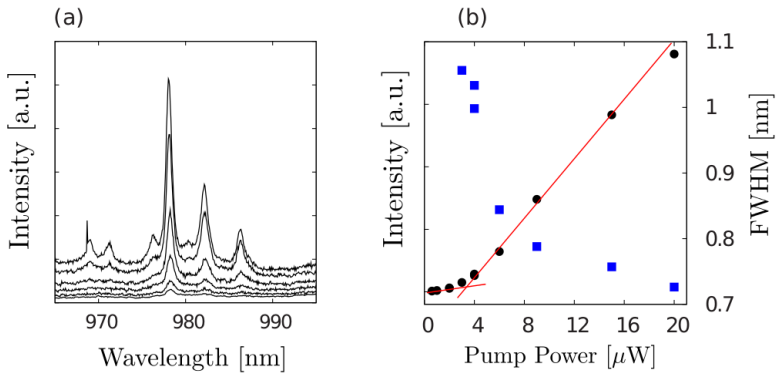

Fig. 17: (a) Emission spectra taken at the incident pump power P=3, 4.1, 6, 9, 15, 20 μW. (b) Measured intensity (black circle) and spectral width (blue square) of one emission peak at wavelength λ= 978 nm vs. P showing the onset of lasing at ~ 3 μW. The red lines are linear fitting of peak intensity below and above the lasing threshold of the device.

In addition, we demonstrated lasing action in quasi-2D Thue-Morse structures *with optimal degree of aperiodicity* fabricated in a GaAs membrane structure [10]. By changing the relative size of two scatterers that correspond to the building blocks *A* and *B*, we gradually vary the degree of aperiodicity and investigate its effect on lasing (Fig. 17). We discovered that there exists an optimal degree of aperiodicity where the quality factor reaches a global maximum and lasing becomes the strongest. This is attributed to an enhancement of horizontal confinement of light in a finite-size pattern by structural aperiodicity. However, the continuous background in the spatial Fourier spectrum of the Thue-Morse structure facilitates vertical leakage of light out of the membrane. At various degrees of aperiodicity, different types of modes acquire the highest quality factors and may be selected for lasing. This work opens a way of controlling lasing characteristic via tuning structural aperiodicity.

Deterministic Aperiodic Structures for on-chip nanophotonics and nanoplasmonics device applications, Award FA9550-10-1-0019

List of project publications

1. C. Forestiere, G. F. Walsh, G. Miano, L. Dal Negro, "*Nanoplasmonics of prime number arrays*", **Optics Express, 17**, 24288 (2009)
2. Gopinath, S.V. Boriskina, S. Selcuk, R. Li, L. Dal Negro, "*Enhancement of the 1.55μm* Erbium emission from quasiperiodic plasmonic arrays", **Appl. Phys. Lett., 96,** 071113 (2010)
3. Forestiere, M. Donelli, G.F. Walsh, E. Zeni, G. Miano, L. Dal Negro, "*Particle swarm optimization of broadband nanoplasmonic arrays*", **Optics Letters 35**, 133 (2010)
4. S. Y. K. Lee, J. J. Amsden, S. V. Boriskina, A. Gopinath, A. Mitropoulos, D. L. Kaplan, F. G. Omenetto, and L. Dal Negro, "*Spatial and spectral detection of protein monolayers with deterministic aperiodic arrays of metal nanoparticles*," **Proc. Natl. Acad. Sci. USA, 107,** 12086 (2010)
5. Svetlana V. Boriskina, Sylvanus Y.K. Lee,Jason J. Amsden, Fiorenzo G. Omenetto and Luca Dal Negro "*Formation of colorimetric fingerprints on nano-patterned deterministic aperiodic surfaces*", **Optics Express, 18,** 14568 (2010)
6. J. Henson, E. Dimakis, J. DiMaria, R. Li, S. Minissale, L. Dal Negro, T.D. Moustakas, R. Paiella, "*Enhanced near-green light emission from InGaAs quantum wells by use of tunable plasmonic resonances in silver nanoparticles arrays",* **Optics Express, 18,** 21322 (2010)
7. J. Yang, S.V. Boriskina, H. Noh, M. J. Rooks, G.S. Solomon, L. Dal Negro, H. Cao, "*Demonstration of laser action in a pseudorandom medium*", Appl. Phys. Lett., **97,** 223101 (2010) **Cover page of APL, November 29**
8. J. Trevino, H. Cao and L. Dal Negro, "*Circularly-symmetric light scattering from nanoplasmonic spirals*", **Nano Lett., 11**, 5, 2008 (2011)
9. L. Dal Negro "*Engineering aperiodic order in nanoplasmonics: past, present, and future opportunities*" to appear in the SPIE Photonics West Conference Proceedings 2011
10. H. Noh, Jin-Kyu Yang, S. V. Boriskina, M. J. Rooks, G. G. Solomon, L. Dal Negro, H. Cao, "*Lasing in Thue–Morse structures with optimized aperiodicity*" **Appl. Phys. Lett**., **98**, 201109 (2011)
11. C. Forestiere, G. Iadarola, L.Dal Negro, G. Miano, "*Near Field Calculation based on the T-matrix Method with Discrete Sources*" to appear in the **J. Quant. Spectrosc. Radiat. Transfer, 112,** 2384 (May 23, 2011)
12. G.F. Walsh, C. Forestiere, L. Dal Negro, "*Plasmon-enhanced depolarization of reflected light from arrays of nanoparticle dimers",* **Optics Express, 19,** 21, 21081 (2011)
13. R. Blanchard, S. V. Boriskina, P. Genevet, M. A. Kats, J. Tetienne, N. Yu, L. Dal Negro and F. Capasso, "*Multi-wavelength mid-infrared plasmonic antennas with nanoscale single focal point",* **Optics Express, 19,** 22113 (2011)
14. R. Blanchard, S. Menzel, L. Diehl, C. Wang, Y. Huang, J.-H. Ryou, R. Dupuis, L. Dal Negro and F.Capasso, "*Multi-wavelength Quantum Cascade Lasers using gratings with an aperiodic basis",* **New Journal of Physics 13**, 113023 (2011)
15. S. F. Liew, H. Noh, J. Trevino, L. Dal Negro, H. Cao, *"Localized photonic bandedge modes and orbital angular momenta of light in a golden-angle spiral"* **Optics Express 19,** 23631 (2011)

16. S. Y. Lee, C. Forestiere, A. Pasquale, J. Trevino, G. Walsh, P. Galli, M. Romagnoli, L. Dal Negro, *"Plasmon-enhanced structural coloration of metal films with isotropic Pinwheel nanoparticle arrays",* **Optics Express 19**, 23818 (2011)
17. S. Minissale, S. Yerci, L. Dal Negro, "*Nonlinear optical properties of low temperature annealed silicon-rich oxide and silicon-rich nitride materials for silicon photonics",* **Appl. Phys. Lett**.,**100**, 021109 (2012)
18. J. Trevino, S.F. Liew, H. Noh, H. Cao, L. Dal Negro "*Geometrical structure, multifractal spectra and localized optical modes of aperiodic Vogel spirals",* **Optics Express, 20,** 3015 (2012)
19. C. Forestiere, A. J. Pasquale, A. Capretti, G. Miano, A. Tamburrino, S. Y. Lee, B. M. Reinhard, and L. Dal Negro, "*Genetically engineered plasmonic nanoarrays",* **Nano Lett.,12** 2037 (2012)
20. E. F. Pecora, N. Lawrence, P. Gregg, J. Trevino, P. Artoni, A. Irrera, F. Priolo, L. Dal Negro "*Nanopatterning of silicon nanowires for enhancing visible photoluminescence"* **Nanoscale**, **DOI:** 10.1039/c2nr30165b (2012)
21. L. Dal Negro, S. V. Boriskina, "*Deterministic aperiodic nanostructures for photonics and plasmonics applications*", to appear in **Laser and Photonics Rev. 6**, 178 (2012)
22. J. Trevino, C. Forestiere, G. Di Martino, S. Yerci, F. Priolo, L. Dal Negro "*Plasmonic-photonic arrays with aperiodic spiral order for ultra thin-film solar cells",* **Opt.Express 20**, A418-A430 (2012)
23. G. Iadarola, C. Forestiere, L. Dal Negro, F. Villone, G. Miano "*GPU-accelerated T-matrix algorithm for light scattering simulations",* **J. Comput. Physics, 231**, 5640 (2012)
24. A. J. Pasquale, B. M. Reinhard, L. Dal Negro "*Concentric necklace nano-lenses for optical near-field focusing and enhancement",* **ACS Nano,** 6, 4341 (2012)
25. N. Lawrence, J. Trevino, L. Dal Negro "*Aperiodic arrays of active nanopillars for radiation engineering",* **J. Appl. Phys., 111,113101 (2012)**
26. A. Capretti, G. Walsh, S. Minissale, J. Trevino, C. Forestiere, G. Miano and L. Dal Negro " *Multipolar Second Harmonic Generation from Planar Arrays of Au Nanoparticles with Aperiodic Order,"* **Opt. Express, 20, 15797 (2012)**
27. L. Dal Negro, N. Lawrence, J. Trevino "*Analytical light scattering and orbital angular momentum spectra of arbitrary Vogel spirals*", **Opt. Express, 20, 18209 (2012)**
28. L. Dal Negro "*Enhancing optical biosensing with aperiodicity"* **SPIE Newsroom,** 16 July 2012, DOI: 10.1117/2.1201206.004306
29. D. Lin, H. Tao, J. Trevino, J.P. Mondia, D.L. Kaplan, F.G. Omenetto, L. Dal Negro, "*Direct transfer of sub-wavelength plasmonic nanostructures on bio-active silk films",* **Adv. Mat.24,** 6088 (2012)
30. E.F. Pecora, T.I. Murphy, L. Dal Negro, "*Rare earth-doped Si-rich ZnO for multiband near-infrared light emitting devices",***Appl. Phys. Lett., 101**, 191115 (2012)
31. N. Lawrence, J. Trevino, L. Dal Negro, "*Control of optical orbital angular momentum by Vogel spiral arrays of metallic nanoparticles",* **Opt. Letters, 37**, 5076 (2012)
32. S. Conesa-Boj, E. Russo-Averchi, A. Dalmau-Mallorqui, J. Trevino, E.F. Pecora, C. Forestiere, A. Handin, M. Ek, L. Zweifel, L. Reine-Wallenberg**,** D. Ruffer, M. Heiss, D. Troadec, L. Dal Negro, P. Carof, A. Fontcuberta i Morral, "*Vertical "III–V" V-Shaped*

Nanomembranes Epitaxially Grown on a Patterned Si[001] Substrate and Their Enhanced Light Scattering", **ACS Nano, 6,** 10982 (2012)

Books

33. *"Optics of Aperiodic Media: Fundamentals and Device Applications"* L. Dal Negro, Cambridge University Press (expected publication 2013)

Book Chapters

34. L. Dal Negro, C. Forestiere, N. Lawrence, S. Y. Lee, J. Trevino, G. Walsh, "*Engineering aperiodic order in nanophotonics",* in Plasmonics: Theory and Applications, edited by Tigran V. Shahbazyan and Mark I. Stockman, **Springer** 2013
35. L. Dal Negro, N. Lawrence, J. Trevino, G. Walsh, "*Aperiodic Order for Nanophotonics",* in Optics of Aperiodic Structrures, edited by L. Dal Negro, **Pan Stanford Publishing** 2013
36. L. Dal Negro, N. Lawrence, J. Trevino, G. Walsh, "*Aperiodic Nano Plasmonics",* in Optics of Aperiodic Structrures, edited by L. Dal Negro, **Pan Stanford Publishing** 2013
37. L. Dal Negro, "*Engineering aperiodic order in nanophotonics",* **Cambridge Univerityv Press** (2013)

Invited Talks:

1. L. Dal Negro, *Enhanced light-matter interactions with engineered photonic-plasmonic nanostructures,* Photonics West SPIE "Photonic and Phononic Properties of Engineered Nanostructures III", 6 February 2013, San Francisco, California USA.
2. L. Dal Negro, *Aperiodic Nanoplasmonics*, MRS Spring meeting 2013, San Francisco, CA, 9-13 April 2013
3. L. Dal Negro, *Current pathways towards silicon-based lasers*, OSA ECOS, 2012, Amsterdam, September 16-20, 2012
4. L. Dal Negro, *Deterministic Aperiodic Nanostructures for Silicon Photonics*, Photonics West, Optoelectronics 2012 Symposium, San Francisco, CA, 21-26 January 2012
5. L. Dal Negro, *Engineering photonic-plasmonic coupling for optoelectronic device applications*, Photonics West, Optoelectronics 2012 Symposium, San Francisco, CA, 21-26 January 2012
6. L. Dal Negro, *Broadband Nanoplasmonics for Energy Harvesting*, 220th Electrochemical Society (ECS) and Electrochemical Energy Summit, Boston, MA, October 9-14, 2011
7. L. Dal Negro, *Aperiodic Nanophotonics: past, present and perspectives*, 4th European Optical Society (EOS) Meeting, Capri, Italy, September 26-28, 2011
8. L. Dal Negro, *Rare earth doping of Si nanostructures: towards optically and electrically pumped lasers*, EMRS Fall Meeting, Warsaw, Poland, September 19-23, 2011
9. L. Dal Negro, *Engineering aperiodic order for optical devices with photonic-plasmonic nanostructures,* SPIE, San Diego, California, 21 - 25 August 2011
10. L. Dal Negro, *Complex Nonperiodic Nanoplasmonics,* IEEE Optical MEMS and Nanophotonics Conference, Istanbul, Turkey, August 8-11, 2011
11. L. Dal Negro, *Light emission from silicon nanostructures: past, present and future perspectives,* 13th International Conference on Transparent Optical Networks ICTON 2011, Royal Institute of Technology KTH, Stockholm, Sweden, June 26 - 30, 2011

12. L. Dal Negro, *Light emission from silicon nanostructures: past, present and future perspectives,* 219th Meeting of the Electrochemical Society, May 1-6, Montreal, QC, Canada, 2011
13. L. Dal Negro, *Waves in a Labyrinth: aperiodic nanophotonics,* First international Conference on "Waves and quantum fields on fractals: recent developments in mathematics, and physics", Lewiner Institute for Theoretical Physics, Technion, June 26-30, Haifa, Israel, 2011.
14. L. Dal Negro, *Engineering aperiodic order for optical devices with photonic-plasmonic nanostructures,* SPIE, San Diego, California, 21 - 25 August 2011,
15. L. Dal Negro, *Rare earth doping of Si nanostructures: towards optically and electrically pumped lasers,* EMRS Fall Meeting, Warsaw, Poland, September 19-23, 2011
16. L. Dal Negro, *Aperiodic Nanophotonics: past, present and perspectives,* 4th European Optical Society (EOS) Meeting, Capri, Italy, September 26-28, 2011
17. L. Dal Negro, *Broadband Nanoplasmonics for Energy Harvesting,* 220th Electrochemical Society (ECS) and Electrochemical Energy Summit, Boston, MA, October 9-14, 2011
18. L. Dal Negro, *Engineered Nanostructures for solar energy conversion,* Photonics West, Optoelectronics 2012 Symposium, San Francisco, CA, 21-26 January 2012
19. L. Dal Negro, "*Engineering aperiodic order in nanoplasmonic devices",* Photonics West, San Francisco, CA, January 22-27, 2011
20. L. Dal Negro, *Aperiodic order for energy harvesting",* Harvesting & Manipulating Light at the Nanoscale Workshop, Molecular Foundry, Berkley, CA, September 30-October 1, 2010
21. L. Dal Negro, *Engineering Light Localization on a silicon chip",* 7th International Workshop on Disordered Systems, Puebla, Mexico, September 20-24, 2010
22. L. Dal Negro, *Engineering Aperiodic Order for Optical Devices with Photonic-Plasmonic Nanostructures",* SPIE Nanoscience and Engineering Symposium, San Diego, California, 1-5 August 2010
23. L. Dal Negro, *Si-based nitride nanostructures: towards optically and electrically pumped lasers, E*MRS Spring Meeting, Strasbourg, France, June 7-11, 2010
24. L. Dal Negro, *Deterministic Aperiodic Structures for Nanophotonics and Nanoplasmonics on-chip Applications,* MRS Spring Meeting, San Francisco, April 5-9, 2010
25. L. Dal Negro, *Engineering Aperiodic Order for Nanophotonics Applications,* March 12, 21010 Kyoto, Japan - International Symposium on Photonic Crystal Structures
26. L. Dal Negro, *Novel concepts in plasmonic sensing,* SPIE BiOS: Biomedical Optics, 23 - 28 January 2010. San Francisco, CA.
27. L. Dal Negro, *Si-based nanoplasmonics,* 2009 Frontiers in Optics Conference/OSA Annual Meeting OSA FiO/LS 2009 Photonics Division October 11-15, 2009, in San Jose, CA, USA.

Contributed Talks:

28. J. Trevino; N. Lawrence; G. Walsh; L. Dal Negro, "*Photon Dispersion and Light Emission from Aperiodic Vogel Spiral Arrays of Dielectric Nanopillars*," Symposium DD: Photonic and Non-linear Devices, MRS Fall Meeting, 11/27/12, Boston, MA.
29. J. Trevino; C. Forestiere; L. Dal Negro, "*Aperiodic Arrays for Broadband Light Absorption Enhancement in Ultrathin-film Silicon Solar Cells*," Symposium K: Hierarchically Structured Hybrid Solar Cells, MRS Fall Meeting, 11/27/12, Boston, MA

30. J. Trevino, C. Forestiere, L. Dal Negro, "*Broadband and wide-angle scattering in aperiodic spiral arrays for ultra-thin film solar cells enhancement*," Silicon-based Nanophotonic Structures, OSA Frontiers in Optics, 10/14/12, Rochester, NY.
31. A. Capretti, G. Walsh, S. Minissale, J. Trevino, C. Forestiere, G. Miano, L. Dal Negro, "*Multipolar Second Harmonic Generation from Plasmonic Arrays*," Dielectric and Plasmonic Periodic Structures and Metamaterials, OSA Frontiers in Optics, 10/14/12, Rochester, NY.
32. E.F. Pecora, N. Lawrence, P. Gregg, J. Trevino, P. Artoni, A. Irrera, F. Priolo, and L. Dal Negro, "*Nanopatterning of optically-active silicon nanowires*," Novel Silicon Waveguides and Nanophotonics, OSA Frontiers in Optics, 10/14/12, Rochester, NY.
33. J. Trevino, S.F. Liew, H. Noh, H. Cao, L. Dal Negro, "*Geometrical structure, multifractal spectra and localized optical modes of aperiodic Vogel spirals*," Focus Session: Nanostructures and Metamaterials, Growth, Structure, and Characterization , APS March, 02/29/12, Boston, MA.
34. A. Capretti, G. Walsh, J. Trevino, G. Miano, L. Dal Nergo, "*Enhanced second harmonic generation from aperiodic arrays of gold nanoparticles*," Focus Session: Nanostructures and Metamaterials, Growth, Structure, and Characterization, APS March, 02/28/12, Boston, MA.
35. N. Lawrence, J. Trevino, and L. Dal Negro, "*Omni-directional active pillar arrays for emission extraction and on-chip generation of optical vortices at 1.55um*," Focus Session: Nanostructures and Metamaterials, Growth, Structure, and Characterization , APS March, 02/29/12, Boston, MA.
36. J. Trevino, N. Lawrence, G. Walsh and L. Dal Negro, "*Engineered Plasmonic-Photonic Arrays for Enhanced Photovoltaics*,"Symposium J: Photonic and Plasmonic Materials for Enhanced Photovoltaic Performance, MRS Fall Meeting, 12/01/11, Boston, MA.
37. J. Trevino, S. Yerci, L. Dal Negro, "*Enhancing photonic-plasmonic interactions on active devices using circular scattering in aperiodic spirals*," Plasmonics: Metallic Nanostructures and Their Optical Properties IX, SPIE NanoScience + Engineering, 08/24/11, San Diego, CA.
38. J. Trevino and L. Dal Negro, "*Engineering Circular Multiple Light Scattering For Polarization-Insensitive Planar Diffraction*," Nanophotonics: Waveguides, Lasers, and SOI-Based Technologies, OSA Integrated Photonics Research, Silicon and Nanophotonics, 6/12/11,Toronto, ON.
39. S. Minissale, J. Trevino, L. Dal Negro, "*Non-linear Optical Properties of Aperiodic Plasmonic Arrays*," Symposium AA: Si/Ge Nanowires, MRS Fall Meeting, 12/01/10, Boston, MA.
40. G. D. Martino, S. Yerci, J. Trevino and L. Dal Negro, "*Plasmon-enhanced Photoconductivity in Thin-film Si Solar Cells*," Symposium AA: Group IV Semiconductor Nanostructures and Applications, MRS Fall Meeting, 11/29/10, Boston, MA.
41. J. Trevino, N. Lawrence and L. Dal Negro, "*Aperiodic Plasmonic Spirals for Light Emission Enhancement in Silicon*," Symposium AA: Group IV Semiconductor Nanostructures and Applications, MRS Fall Meeting, 11/29/10, Boston, MA.
42. N. Lawrence, J. Trevino, L. Dal Negro, "*Aperiodic Arrays of Active Nanopillars for Si-based Light Emission*," Symposium AA: Photonic Crystals, MRS Fall Meeting, 12/01/10, Boston, MA
43. S. V. Boriskina, J. Trevino, B. Yan, L. Yang, B. Reinhard and L. Dal Negro, "*Planar Multi-band Optical Nanoantennas with Nanoscale Spatial Resolution*," Symposium M: Resonant Optical Antennas--Sensing and Shaping Materials, MRS Fall Meeting, 12/01/10, Boston, MA.

44. J. Trevino, N. Lawrence, and L. Dal Negro, "*Fabrication and Dark-Field Scattering Characterization of Deterministic Aperiodic Plasmonic Spirals*," Plasmonics, OSA Frontiers in Optics, 10/24/10, Rochester, NY.

Invited Seminars:

45. L. Dal Negro, "*Materials and fields at the nanoscale: engineering coupled resonances for planar optical devices*", University of Vanderbilt, January 23, 2013
46. L. Dal Negro, "*Engineering photonic-plasmonic coupling in metal-dielectric nanostructures*", University of Trento, Italy, November 09, 2012
47. L. Dal Negro, "*Engineering photonic-plasmonic coupling in metal-dielectric nanostructures*", CNR-NANO, University of Modena & Reggio, Italy, November 05, 2012
48. L. Dal Negro, "*Nano-Si light emission in a (thin)nutshell*", KTH – Stockholm, Sweden, October 12, 2012
49. L. Dal Negro, "*Engineering photonic-plasmonic coupling in metal-dielectric nanostructures*", KTH – Stockholm, Sweden, October 9-14, 2012
50. L. Dal Negro, "*Bio-inspired Nanophotonics*", AIChE Biomimicry Meeting 2011, Boston, MA, November 04, 2011
51. L. Dal Negro, "*Engineering Aperiodic Order in Nanoplasmonics*", European Laboratory for Nonlinear Spectroscopy (LENS) – Florence, Italy, May 10, 2011
52. L. Dal Negro, "*Broadband Nanoplasmonics: Enhancing light-matter coupling at the nanoscale*", US Army Natick Soldier RDE Center – April 20, 2011
53. L. Dal Negro, "*Photons in a Labyrinth: challenges & opportunities of aperiodic nanophotonics*", University of Toronto, Toronto, Canada, March 24, 2011
54. L. Dal Negro, "*Photons in a Labyrinth: challenges & opportunities of aperiodic nanophotonics*", Brown University, Providence, RI, September 17, 2010
55. L. Dal Negro, "*Photons in a Labyrinth: challenges & opportunities of aperiodic nanophotonics*", ARL-Multiscale Modeling Workshop, Fairfax, VA, Sept. 1-2, 2010
56. L. Dal Negro, "*Engineering aperiodic order in nanophotonics: past, present and future opportunities*", Max Planck Institute, Erlangen, Germany, May 12, 2010
57. L. Dal Negro, "*Engineering optical interactions in complex photonic-plasmonic nanostructures*", Wesleyan University, 2010 February 25, Middletown, CT, USA
58. L. Dal Negro, "*Engineering Light Waves in Aperiodic Media*", Lectio Magistralis, University of Trento, Italy, January 27, 2010
59. L. Dal Negro, "*Engineering aperiodic structures: from algorithmic botany to light localization*", Tufts University, October 26, 2009
60. L. Dal Negro, "*Engineering Aperiodic Structures for on-chip nanophotonics applications*", Stanford University, October 19, 2009
61. L. Dal Negro, "*Light in aperiodic systems*" Harvard University, October 09, 2009
62. L. Dal Negro, "*Light in deterministic aperiodic media*" Queens College, NY, October 05, 2009